Remote sensing, geophysics and imaging technology for monitoring and characterization of geostructures and geo-materials

Thi Minh Hue Le, Jean-Sébastien l'Heureux, Victor Hopman, Georgia Giardina, Malte Vöge, Regula Frauenfelder, Suzanne Lacasse, Stanislav Lenart, Angel Tijera Carrion, Ruben Ruiz Bravo, et al.

Deliverable D 09.04

Remote sensing, geophysics and imaging technology for monitoring and characterization of geo-structures and geo-materials

Version 1.1
14.10.2022

GEOLAB

Project Information

Project acronym	GEOLAB	
Project title	Science for enhancing Europe's Critical Infrastructure	
Grant agreement number	101006512	
Start date / Duration	1 February 2021	48 months
Project partners	Deltares, TU Delft, ETHZ, UM/ZAG, TUDa, NGI, CEDEX, Uni Eiffel, UCAM, KPMG	

Document Information

Work Package title	JRA2: Innovation to enhance capabilities of GEOLAB	
Deliverable title	D9.4 Remote sensing, geophysics and imaging technology for monitoring and characterization of geo-structures and geo-materials	
Document type	Report	
Doc. version & WP no.	1.1	WP 9
Lead author(s)	Thi Minh Hue Le (NGI), Jean-Sebastien L'Heureux (NGI)	
Contributing author(s)	Victor Hopman (Deltares), Giorgia Giardina (TU Delft), Malte Voge (NGI), Regula Frauenfelder (NGI), Suzanne Lacasse (NGI), Stanislav Lenart (ZAG), Ángel Tijera Carrión (CEDEX), Rubén Ruiz Bravo (CEDEX), Evangelia Korre (ETH-Z), Ioannis Anastasopoulos (ETH-Z), Zheng Li (Uni Eiffel), Luc Thorel (Uni Eiffel), Alain Neel (Uni Eiffel), Matthieu Blanc (Uni Eiffel), Thierry Dubreucq (Uni Eiffel), Sam Stanier (UCAM), Haitao Lan (UCAM)	
Reviewer(s)	Victor Hopman (Deltares), Stefano Muraro (TU Delft), Huan Wang (TU Delft), Sam Stanier (UCAM)	
Release date	14.10.2022	

Classification – This report is:									
Draft		**Final**	x	**Public**	X	**Restricted**		**Confidential**	

Revision history			
Version	**Release Date**	**Status**	**Distribution**
0.0	12.09.2022	Draft	Consortium
1.0	23.09.2022	Draft	Coordinators reviewer
1.1	14.10.2022	Final	Project Officer

Acknowledgment

This project has received funding from the European Union's Horizon 2020 research and innovation programme under grant agreement No. 101006512.

Disclaimer

Executive Summary

Climate change, extreme events and aging are causing and/or accelerating numerous geotechnical challenges such as geohazards and deformation/settlement of buildings and infrastructure. In addition, increasing demand and pressure on the built environment stimulate the need for innovative methods/equipment for characterization of ground condition and detection of objects, utilities, defects which can interfere with construction/maintenance of infrastructure. Remote sensing, geophysical methods and imaging technologies offer great potential for innovative and cost-effective approaches for monitoring of critical infrastructure, characterization of sub-surface spaces and detection of ultilities, objects and defects. Their main advantages are that they are non-intrusive / non-destructive, fast and have the possibility to cover large areas and challenging terrain; something that is costly or impossible if using traditional methods.

Remote sensing, geophysical techniques and imaging technology have been utilised in physical modelling at different scales, from small laboratory studies to large scale field testing. This report provides overviews of remote sensing, geophysical methods and image analyses which are suitable for monitoring infrastructure or ground characterization or detection problem. This report focuses on technologies and methods that have been utilized by partners in the GEOLAB consortium. For each method, a brief overview of key principles, advantages / disadvantages and / or applicability is provided, followed by examples of application of the method in real projects delivered by GEOLAB consortium partners.

Many GEOLAB partners had or have ongoing research and development activities which utilize one or more remote sensing, geophysical methods or imaging technology in innovative physical modelling, small laboratory experiment, medium lab-field test or large/full-scale field testing. Most of the applied technologies have reached TRL 6-7, thus they have been or are applicable in real operational environment. Some of the example applications presented in this report are performed in practical industry projects (e.g. road construction, dam monitoring).

There is, however, a great need to further develop modelling techniques in the laboratory and in the field, as well as research into data processing methods to optimize their applicability in geo-engineering challenges. In addition, there is a need for more real-world cases demonstrating the advantages and cost-effectiveness of these methods, so as to encourage their usage in practice. There is great potential for collaborative research amongst the GEOLAB partners and Transnational Access user groups, hence the purpose of this report is to provide an overview of current remote sensing, geophysical methods or imaging analysis capabilities in physical modelling, laboratory tests or field tests within the GEOLAB consortium, in order to promote collaboration and innovation.

CONTENTS

List of Tables

List of Figures

1 Introduction

1.1 About GEOLAB

The existing Critical Infrastructure (CI) of Europe in the water, energy, urban and transport sector is facing major challenges because of pressures such as climate change, extreme events, geo-hazards, aging and increased usage in combination with pivotal changes in the CI to meet long-term societal goals (e.g. energy transition). To address these challenges, scientific research and innovative solutions are needed that can only be achieved by an interdisciplinary, cross-boundary approach and by equipping expert teams with the most advanced suite of physical research infrastructure available that allows them to work across spatial scales, explore different theories that describe the pressures and adopt innovative techniques for solutions.

The GEOLAB Research Infrastructure (RI) consists of 11 unique installations in Europe aimed to study subsurface behaviour and the interaction with structural CI elements (e.g. a bridge) and the environment. The overarching aim of GEOLAB is to integrate and advance these key national research facilities towards a one-stop-shop of excellent physical RI for performing ground-breaking research and innovation to address challenges faced by the Critical Infrastructure of Europe.

During the Joint Research Activities (JRA), the capabilities of the integrated GEOLAB RI services are improved beyond present state-of-the-art. Topics are: (1) Harmonizing operation (2) Advancing physical modelling of the impact of climate change, aging and extreme events on CI; (3) Development of 3D-4D measurement techniques; (4) Application of new materials and new sensing techniques; (5) Data management of performed experiments for future re-use.

During Transnational Access (TA), users outside the consortium gain access to the GEOLAB installations to perform research and innovation. The scientific research community will use the enhanced capabilities of GEOLAB from the JRA to perform ground-breaking experiments. For CI managers and policy makers, the activities will result in a more comprehensive understanding of the challenges facing CI and evidence to base decision making upon. The construction industry will use GEOLAB to proof innovative solutions for the CI and so gain more leadership in the industrial and enabling technologies.

There will be close interaction with Small and Medium-sized Enterprises (SME) that develop user-friendly engineering software from numerical modelling advances which are validated in the TA projects. We will explicitly challenge SME on sensing, new materials and other niches for innovative solutions, which will have spinoff in other fields of application, contributing to the competitiveness of Europe.
Networking Activities (NA) are another core element of GEOLAB, culminating in workshops and other outreach events that foster a digital and In Real Life community, thereby providing a productive channel to communicate with different stakeholder groups.

The GEOLAB consortium is a collaboration of renowned organizations coordinated by Deltares (the Netherlands). Other consortium partners are: CEDEX Spain, NGI Norway, University of Cambridge (United Kingdom), Delft University of Technology (the Netherlands), University of Maribor (Slovenia), Technical University Darmstadt (Germany), ETH Zürich (Switzerland), Université Gustave Eiffel (France) and KPMG Future Analytics (Ireland).

More information: www.project-geolab.eu.

1.2 Joint Research Activities (JRA)

The Joint Research Activities (JRA) are an essential element of GEOLAB and contribute significantly to the declared overarching goal of the project by aiming for the following subordinate goals:

- Synergetic integration of experimental research infrastructure in the disciplines of subsurface behaviour (soil mechanics and hydrogeology), engineering (geotechnical, structural, engineering geology and environmental) and data science (ICT, advanced data analyses and virtual access)
- Improvement of physical modelling and measurements techniques beyond present state-of-the-art that facilitate studying complex and interdisciplinary effects.
- Provision of guidance on and integration of data management methods (standardization); set-up of an open access database of well-documented experiments for efficient data exchange between installations and re-use of experiment data sets.

Consequently, JRAs are crucial to create synergy and stimulate innovation of the GEOLAB RI beyond present state-of-the-art. In alignment with the previously mentioned subordinate goals, JRAs comprise the following components:

- JRA1 “Guidance” improves and harmonizes the operation of our installations by conducting an inventory of the installations and development of GEOLAB user’s manual, among others.
- JRA2 “Innovation” enhances the capabilities of GEOLAB by: (a) advancing physical modelling of the impact of climate change, aging and extreme events on CI; (b) developing 3D-4D measurement laboratory and field techniques; (c) using new materials and applying new sensing techniques.
- JRA3 “Data management” offers virtual access to a database of performed experiments that is suitable for future re-use of data and easy comparison across installations.

GEOLAB will disseminate achievements of the JRA work packages through journals publications, national and international conferences, workshops, as well as through other communication channels such as social media, website and personal contacts. The results of JRA1 “Guidance” will be published on the project website as valuable information to potential new users, new generation (NG) researchers, other laboratories and academia. JRA2 “Innovation” will display advances of the GEOLAB infrastructure and demonstration projects that highlight the interaction between physical and numerical models and between physical models and the environment. Finally, JRA3 “Data management” offers virtual access to a database of performed experiments that will become available to all stakeholders to allow for re-use of data.

1.3 Aim and approach of Deliverable 9.4

In recent decades, the design, monitoring and maintenance of Europe's CI has benefited from significant technological advances in the field of remote sensing, geophysics and image analyses. Both data acquisition methods, processing and interpretation tools, and imaging technologies have evolved considerably. Remote sensing, imaging technology and geophysical survey can be cost-effective methods that allow non-invasive/non-destructive measurements and/or 2D and 3D imaging of surfaces and sub-surfaces, particularly over large areas. Measurements can be acquired in real-time to evaluate and monitor material and structural changes, and thus the safety of a given structure over time. Better integration of remote sensing, geophysical techniques and imaging technology with measured physical data locally offer great potential for optimizing and improving the efficiency of Europe's geo-engineering monitoring systems and characterisation technology.

Remote sensing, geophysical techniques and imaging technology have been utilised in physical modelling at different scales, from small laboratory studies to large scale field testing. This report provides overviews of remote sensing, geophysical methods and image analyses which are suitable for monitoring infrastructure or ground characterisation. This report focuses on technologies and methods that have been utilized by partners in the

GEOLAB consortium. in order to facilitate integration of infrastructure and collaboration of expertise among GEOLAB partners and with GEOLAB community.

For each technology/method presented in this report, a brief overview of key principles, advantages/disadvantages and/or possible applications is provided, followed by presentation of different projects in which the technology or method has been utilised by GEOLAB partners. A conclusion with possibilities for future work is included.

There is great potential for collaborative research amongst the GEOLAB partners and Transnational Access user groups, hence the purpose of this report is to provide an overview of current remote sensing, geophysical methods or imaging analysis capabilities in physical modelling, laboratory tests or field tests within the GEOLAB consortium, in order to promote collaboration and innovation.

2 Remote sensing technologies

Victor Hopman
Deltares, Netherlands

Giorgia Giardina
Delft University of Technology, Netherlands

Malte Voge, Regula Frauenfelder, Suzanne Lacasse, Jean-Sebastien L'Heureux, Thi Minh Hue Le
Norwegian Geotechnical Institute, Norway

2.1 Background

European critical infrastructures such as roads, railways, buildings, power plant, pipelines are susceptible to both natural disasters (e.g. floods, erosions, landslides) and manmade threats (e.g. war, terrorism, construction accidents). Remote sensing technology has already contributed to diagnosing and detecting problems in vital infrastructures effectively. Space-borne measurements enable not only prediction of where and when a particular hazard may occur, but also whether or not it will have significant socio-economic consequences. This is of great significance in reducing downtime and to mitigate serious negative societal impacts.

Remote sensing is the process of detecting and monitoring the physical characteristics of an area by measuring its reflected and emitted radiation at a distance (typically from satellite or aircraft)(USGS, 2022). Special cameras collect "remotely sensed" images which are analysed to learn about certain target areas and the on-going changes in the environment (USGS, 2022). The use of remote sensing techniques has rapidly grown worldwide over the last few decades due to the development of sensors and satellites. Particularly, emerging satellite technology enabled the development of a number of interesting techniques to monitor changes on the Earth's surface.

Remote sensors can be classified as either passive or active sensors (Figure 1). Passive sensors collect radiation from the Sun that are reflected by the object or surrounding areas. Examples of passive remote sensing technologies include radiometers, spectrometers, imaging radiometers and accelerometers. Active sensors emit energy to scan objects/areas, and the sensor detects and measures the reflected radiation from the target. Active remote sensors transmit either light or waves and can measure distances or heights. The most well-known examples of active remote sensing are radars and lidars. Radar is a sensor that emits radio signals and measures the amount of reflection, traveling time and phase. Lidar transmits light impulses and measures the quantity retrieved.

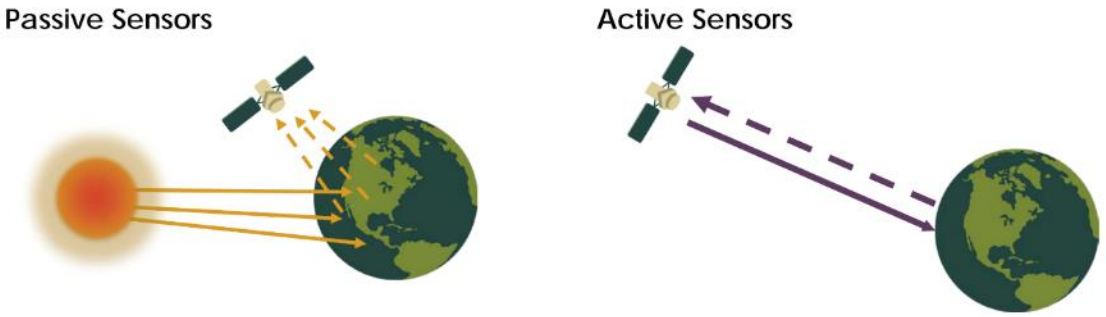

Figure 1. Diagram of a passive sensor versus an active sensor. Credit: NASA Applied Sciences Remote Sensing Training Program (Source: earthdata.nasa.gov).

Active remote sensing technologies such as satellite-based radar interferometry (InSAR), Light Detection and Ranging (LiDAR) have been tested and used in the field by a number of the GEOLAB consortium partners. This section presents overview of these two technologies and examples of their application.

2.2 Satellite-based radar interferometry – InSAR

Overview

Synthetic Aperture Radar (SAR) is a radar imaging system that sends radar waves to the Earth's surface from a satellite. A continuous band-shaped image is obtained by processing the energy reflected from objects on Earth. The distance between satellite and object can be determined based on the time signature of a signal received by the SAR antenna. The accuracy of this distance is in the order of several meters. The resolution of the SAR system determines the dimensions of the pixel (resolution cell in Figure 2). This is the area whose reflection data is captured in one individual pixel. Multiple reflectors can be present in one pixel. The measurement of the displacement of the pixel is possible by interferometry, hence the name InSAR (Interferometric Synthetic Aperture Radar).

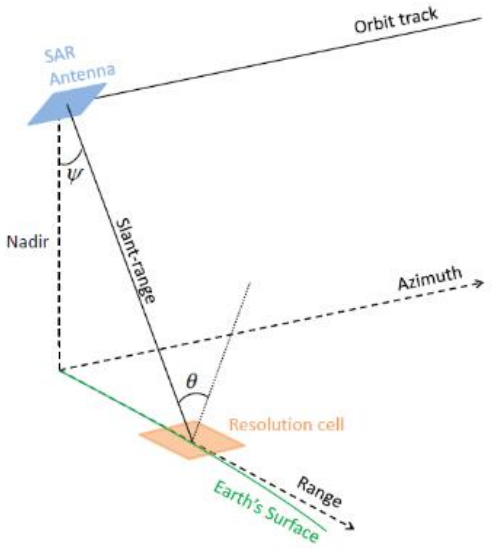

Figure 2. Geometry of a SAR system (Image: Deltares)

InSAR is capable of determining surface deformations in the line-of-sight (LOS) direction of a sensor, by pairing SAR images of the same scene acquired at different points in time. The method relies on identifying coherent scatterers, i.e. objects that remain recognizable in the radar signal throughout the temporal analyses window, even though they might slowly deform or move. In most areas, potential targets are relatively stable over time, and it is possible to find a large number of naturally occurring scatter points (for example, fixed objects like buildings, large boulders etc). Radar images acquired by orbiting satellites at different times are compared to derive the difference in phase and amplitude of the radar signal. From this difference the relative displacement of the monitored objects between two acquisitions can be calculated, with a centimetre to millimetre accuracy. The result is a high-resolution estimate of deformation at these points, with a precision better than 1 mm/year along the sensor — target line of sight.

There are various factors that determine the phase difference between the two observations by InSAR. Determining the contribution of the distortion of the pixel to the phase difference requires correction for various factors. Depending on the complexity of the solution, these factors have been considered to a greater or lesser extent in the correction:

- Difference in the position of the satellite between the two observations;
- Topography;
- Deceleration in the atmosphere; for example, by particles in the atmosphere;
- Errors in satellite orbit determination;
- Changes in the reflection properties of the pixel, for example between greenery, city and water;
- Different sources of noise, for example the uncertainty of the measuring instrument; and

- Difference in the number of wave cycles between the two observations.

The distortion of the pixel in the viewing direction of the satellite can be determined from the remaining phase difference: the 'line-of-sight' distortion. The horizontal and vertical components of the line-of-sight deformation can be estimated by combining the deformation vector of observations in the ascending and descending orbits, and an estimate of the main direction of the horizontal deformation.

The use of InSAR observations is limited by changes in the reflective properties of the pixel over time and the different viewing directions of the two satellite observations. Time series analysis uses the interference patterns of several observations over time to better determine the different contributions to the phase difference. The reliability of a time series strongly depends on the phase unwrapping of the observations. Phase unwrapping is the determination of the correct difference in the number of wave cycles between the two observations. Usually there is no unique solution for the phase unwrapping and additional assumptions have been made during the processing for the following factors:

- Presence of noise;
- Variations in the effect of the atmosphere on the phase difference;
- Smoothness of the deformation of the pixel in time or space: large deformation differences in time; or location of the reflectors in the pixel.

The contribution of all individual reflectors ('scatterers') in the pixel determines the total reflection of the cell. If there is one prominent scatterer in the cell, it largely determines the phase of the reflected signal. The presence of such a persistent scatterer (PS) significantly strengthens the coherence of observations at different times. If the pixel does not contain a persistent scatterer, the phase is determined by different scatterers and the cell is a distributed scatterer (DS) (Figure 3). Persistent scatterer interferometry is based on the detection and analysis of the deformation of persistent scatterers in a time series analysis (Leijen, 2014). Reliable measurements of deformations in urban areas are possible because structures often cause strong reflections.

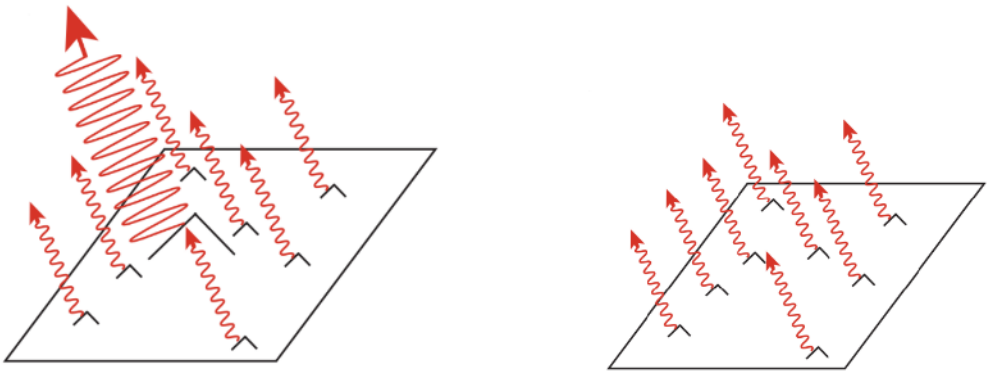

Figure 3. Reflection characteristics of a persistent scattering pixel (left) and a distributed scattering pixel (right) (Image: Deltares)

InSAR data have been traditionally used to investigate geological processes like glaciers, landslides, earthquakes, volcanos. The recent availability of high-resolution X-band spaceborne SAR constellations (Milillo et al., 2016) has enabled the use of InSAR techniques as a cost-effective tool for long-term, near-real time monitoring of buildings, infrastructure and geo-hazards (Giardina et al., 2019, Milillo et al., 2019, Macchiarulo et al., 2022). InSAR is a powerful tool for measuring displacements of the Earth's surface that can provide measures of Earth surface displacements in all weather conditions, by day or night, for geographically extended areas and at relative low-cost (Hanssen, 2001). It has been ultilized widely in tackling geo-hazards such as settlement due to groundwater exploitation, and the impacts of underground mining activity or tunnelling to name just three. In the past, it has mostly focused on post analyses and monitoring of slope deformation, but the technique is now extended to early warning applications (Schlögl et al., 2022).

Recent development in InSAR data processing have shown that the L-band data (ALOS PALSAR, NISAR) are much less influenced by vegetation cover (Jebur et al., 2014, Nishiguchi et al., 2017). In 2023, the launch of NISAR, an

American-Indian L- and S- band SAR satellite is expected. NISAR will observe the earth's land areas globally with a 12-day repetition interval and a spatial resolution between 3-10 m, depending on the mode. In 2024, the ESA satellite Rose-L (Sentinel-12) will begin delivering L-band data across the globe, with a planned global coverage every 6 days and a spatial resolution of 5 x 10 m. Such technology will provide new and unique possibilities enabling real time monitoring of changes, for example, in potential aggravating factors (e.g. erosion, urbanisation) for the stability of slopes. However, there is a need to develop algorithms, methodologies and training of scientists in the use of L-band SAR data.

The main challenges of InSAR applications for structural and geo-hazard monitoring are connected to the need to verify the data availability and consistency for the specific area of interest, the niche expertise required for data processing and interpretation, and the difficulty in decomposing measurements that are provided along the satellite line of sight, as opposite to horizontal-vertical directions (Macchiarulo et al., 2022).

To summarise, key points about InSAR technologies that should be considered prior to deployment include:

1. InSAR measurements are relative: the first measurement in a measurement series is the zero point. To make the InSAR measurements absolute, calibration to a terrestrial measurement at the same point is necessary. For this reason, InSAR measurements are most suitable for determining strain rates and strain accelerations. Usability should be reviewed for each application.
2. The main limitation of the InSAR technique for early warning is the repetition time of the measurements (currently at least 11 days, depending on the satellite) in combination with the random deviation between successive measuring points. The random deviation of individual observations from the trend depends on the standard deviation of the deviation of the observations from the trendline. This means that deviating behavior such as the increase in the deformation rate only becomes clear if several successive measuring points systematically deviate from the previous trend. In a few years, new satellites will provide InSAR data with a repetition time of a few days. The random deviation can then be reduced.
3. Another limitation of the InSAR technique as a means of surveillance monitoring is that it is difficult to detect large settlement rates. If the settling of an object between two passes of the satellite is greater than 10 to 15 mm (half the wavelength of the X-band satellite signal) it is difficult to determine whether the settling is real or an artefact of the InSAR processing.
4. The large amount of InSAR data means that it is possible to have automatic detection. For example, analyzing trend breaks in the data: jumps in the individual time series, changes in the noise around the trendline. In that process of automation, the data analyst makes choices that can determine the outcome. Despite the large amount of points from InSAR, the location of the individual reflection points cannot be determined in advance.

Application of InSAR to the monitoring of tailing dams

Partner: Norwegian Geotechnical Institute (NGI)

The failure of tailing dam can have catastrophic consequences; thus monitoring is critical to sustainable mining practice. Satellite-based radar interferometry (InSAR) constitutes an innovative method for field monitoring of tailings dams. To assess the feasibility of satellite-based radar interferometry (InSAR) for monitoring tailings dams, two case studies were conducted by the NGI. Ground displacements mapped by InSAR were analysed in these cases: the Feijão Mine tailings dam in Brazil and the Zelazny Most tailings dam in Poland. For both cases, data from the Sentinel-1 radar satellite constellation were obtained from the EU Copernicus Programme.

Two different processing methods, Persistent Scatterers – PS (Ferretti et al., 2000) and Small Baseline Subset Algorithm – SBAS (Berardino et al., 2002), were applied and compared. For both dams, the SBAS method provided better coverage, but the measurements close to the crest of the dam seemed to be adversely affected by the spatial filtering, which "smeared" the high displacement velocities of the beach tailings onto the dam.

Figure 4 gives an example of results from time series analyses of InSAR data for three areas on the Feijão Mine tailings dam in Brazil before the failure occurred on the 25th of January 2019. The figure shows the velocity map for the SBAS processing method. The largest displacement rates were observed along the beach, close to the crest

of the dam, which is likely related to the tailings settlements. Along the crest and the upper part of the dam, the measurements indicated an average displacement rate of about 15 mm/year in line-of-sight, corresponding to a downslope movement. With -10 mm/year, the lower part of the dam showed less movement. This is expected for a dam constructed with the upstream construction method, as the upper part of the dam will be supported by thicker layers of soft tailings. A smaller part in the centre of the dam face appeared to show an increased downward movement following December 17, 2018. This could indicate- a precursor of the upcoming failure. However, as this increase in velocity is only covered by three acquisitions, the signal should be interpreted with great care, and comparisons with ground-based measurements would be necessary to conclude whether the InSAR method was able to capture the increase in the velocity just before failure in this case (Vöge et al., 2022).

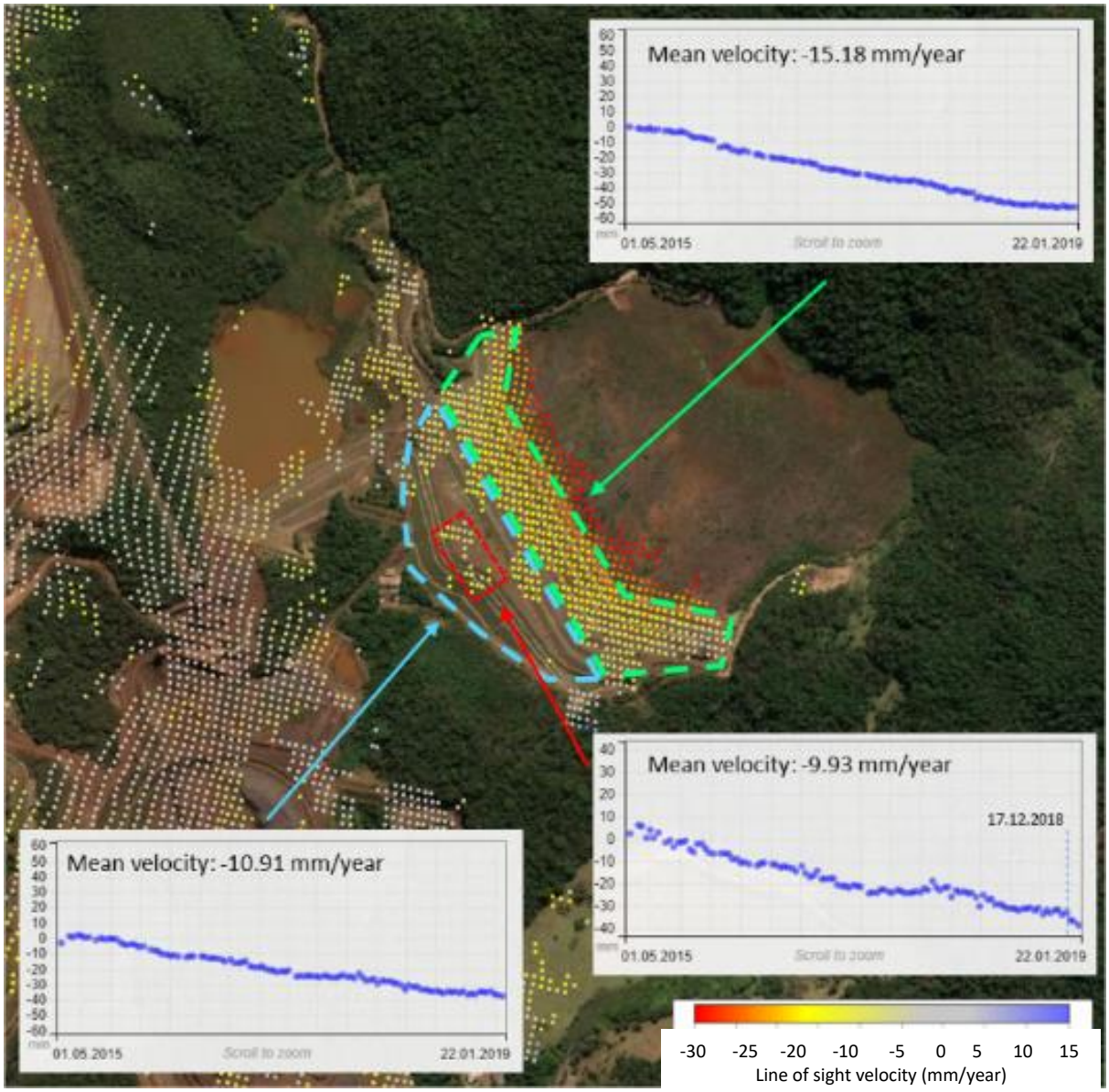

Figure 4. Line-of-sight displacements at the Feijão Mine tailings dam B-I from May 2015 to just before failure January 25, 2019 (displacements averaged over time in each outlined area (Vöge et al., 2022)

For the Zelazny Most dam, data from two different acquisition geometries were analysed, which allows the decomposition of the horizontal and vertical displacements from the line-of-sight displacements (Figure 5 and Figure 6). This was performed for the data processed with the SBAS method. The vertical displacements (Figure 6, left) showed a pattern that was very similar to the corresponding line-of-sight

displacement (Figure 5, left). Along the eastern flank of the dam, at the lower part of the dam face, the vertical displacement values are smaller compared to the line-of-sight displacement. Therefore, a horizontal displacement component, directed outward, is observed (Figure 6, right). The same can be observed on the western side of the dam. The PS method provided more accurate measurements, but the coverage with measurements on the dam slopes was sparse (Figure 5, right) (Vöge et al., 2022). The study shows that InSAR technology can be innovative effective tools for monitoring of tailing dams or similar structures, but cross-validation with measurement from other methods are necessary to ensure accurate interpretation of the results.

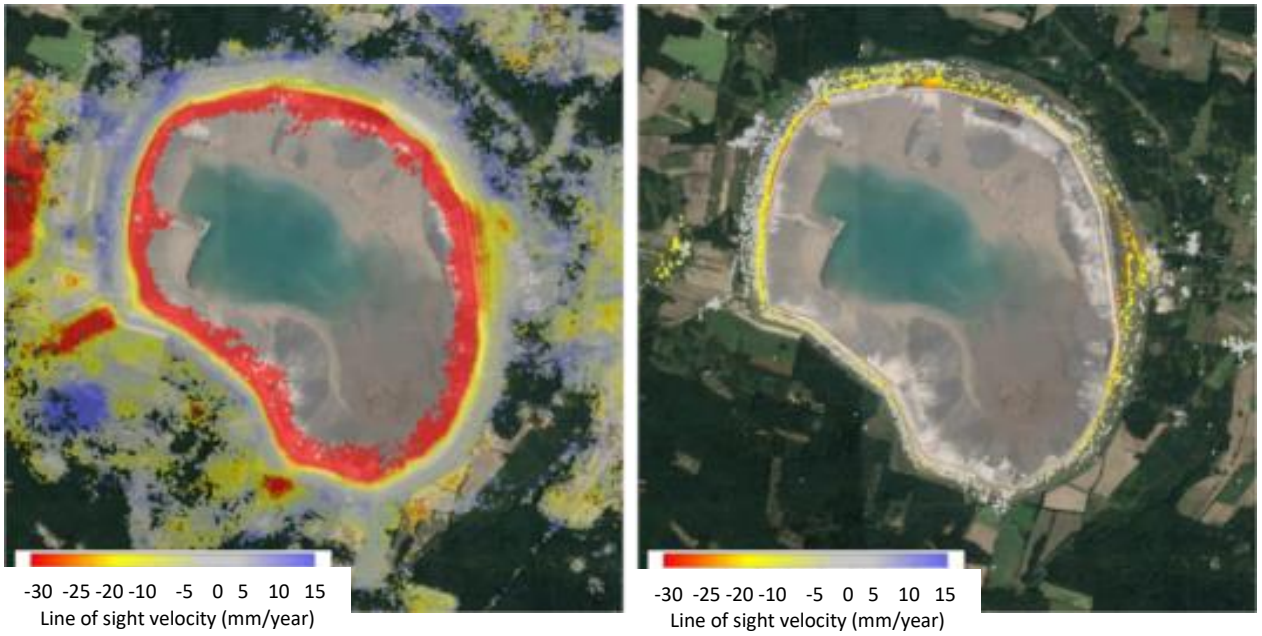

Figure 5. Displacements measured by InSAR at Zelazny Most. Left: SBAS results in line-of-sight; Right: PS results in line-of-sight (Vöge et al., 2022).

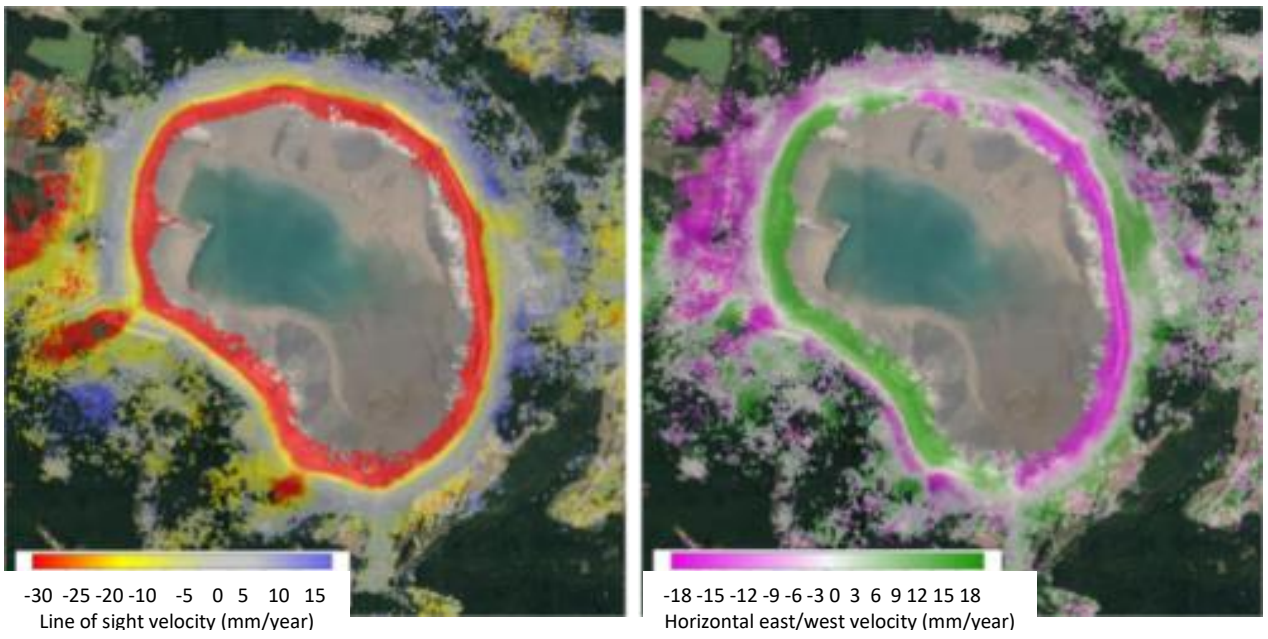

Figure 6. Vertical (left) and horizontal east-west (right) velocity maps (Zelazny Most): Negative values (red) represent settlements, positive values (blue) represent heave; Negative values (pink) represent westward movement, positive values (green) represent eastward movement (Vöge et al., 2022).

Application of InSAR to the monitoring of tunnelling-induced settlement

Partner: Delft University of Technology (TUDelft)

The application of InSAR-based monitoring to assessment of tunnelling-induced deformations of buildings was explored by Giardina et al. (2019) the methodology was tested on a 25 km^2 area between Paddington and Liverpool Street along the Crossrail twin tunnel route in London, producing a dataset comprising of 72 COSMO-SkyMed images acquired from April 2011 to December 2015. These were subsequently combined to produce a time-series of cumulative deformation over the city of London (UK), covering the area where the Crossrail twin tunnels were excavated from 2012 onwards (Figure 7). After a comparison between traditional and InSAR monitoring data for the London area during the Crossrail excavation, the high resolution, high density InSAR-based displacements were used to evaluate the building deformations for a number of case studies. Results showed how the InSAR time-series product can overcome the lack of ground-based monitoring of building displacements and thus facilitate the application of damage assessment procedures which take the soil-structure interaction mechanism into account (Figure 8).

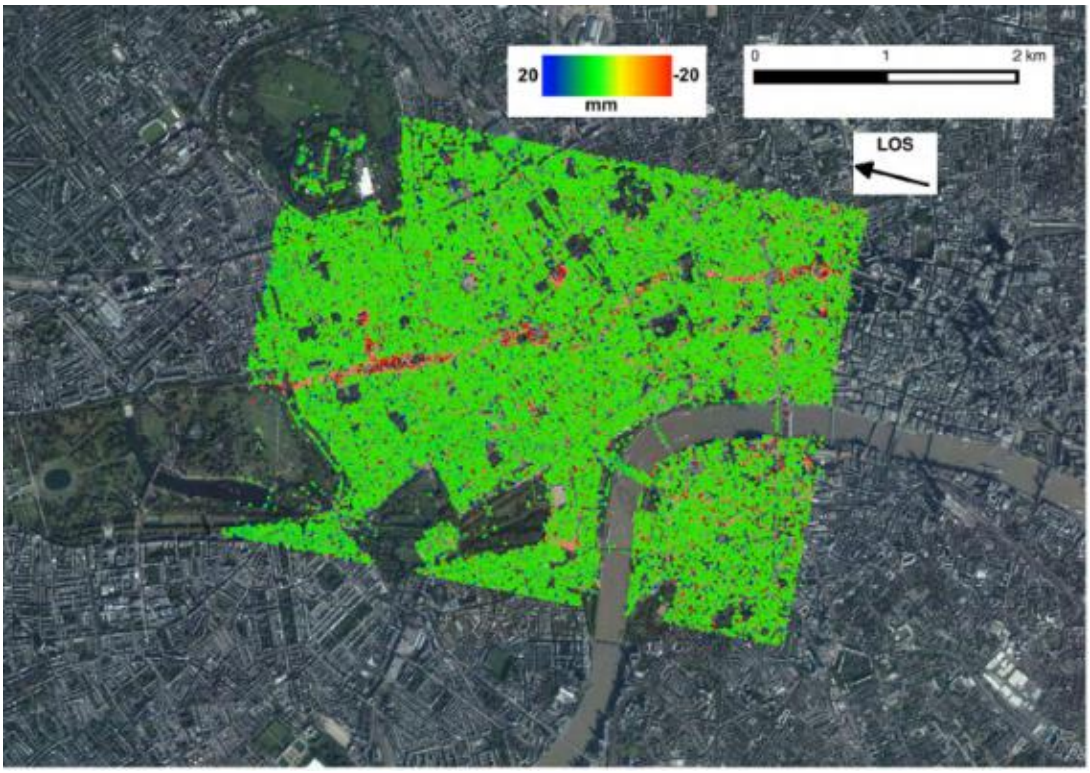

Figure 7. Cumulative displacement map over London spanning April 2011–December 2015 (Giardina et al., 2019). Negative values indicate targets moving away from the satellite. Blue stars indicate the locations of the analysed buildings.

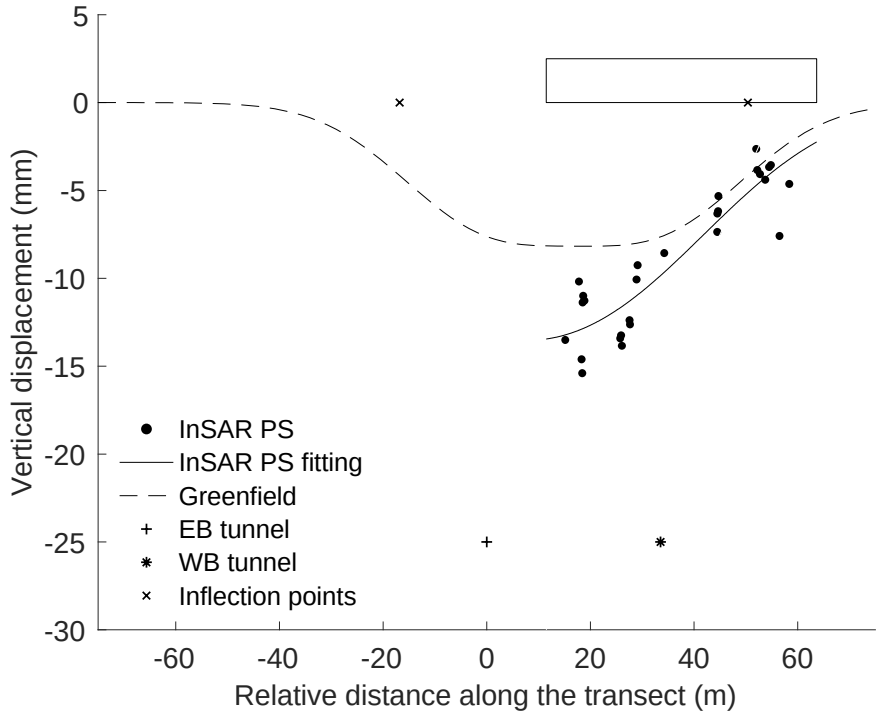

Figure 8. Example of InSAR-based displacements measured at the top of a building (Giardina et al., 2019).

Application of InSAR to the monitoring of transportation infrastructure network

Partner: Delft University of Technology (TUDelft)

InSAR-based monitoring can provide an overview of the state of transportation infrastructure networks at regional scale and identify potential damage precursor. In Macchiarulo et al. (2022), a fully automated integration between GIS data and InSAR time-series has been applied to road networks in California and Italy to detect potential hazards. The integrated methodology automatically processes large volumes of PS displacement time-series and road network GIS inventories to extract deformation data over a given network (Figure 9), and performs local deformation analysis designed to detect anomalous differential movements between parts of the same piece of infrastructure (Figure 10). A Sentinel dataset from 2016 to 2019 was used to analyse the Los Angeles highway and freeway network, while the Italian motorway network was evaluated by using open access ERS/Envisat datasets between 1992 and 2010, COSMO-SkyMed datasets between 2008 and 2014 and Sentinel datasets between 2014 and 2020. The outcomes highlighted the potential for InSAR techniques to be integrated into structural health monitoring systems and improve current procedures for transport network management.

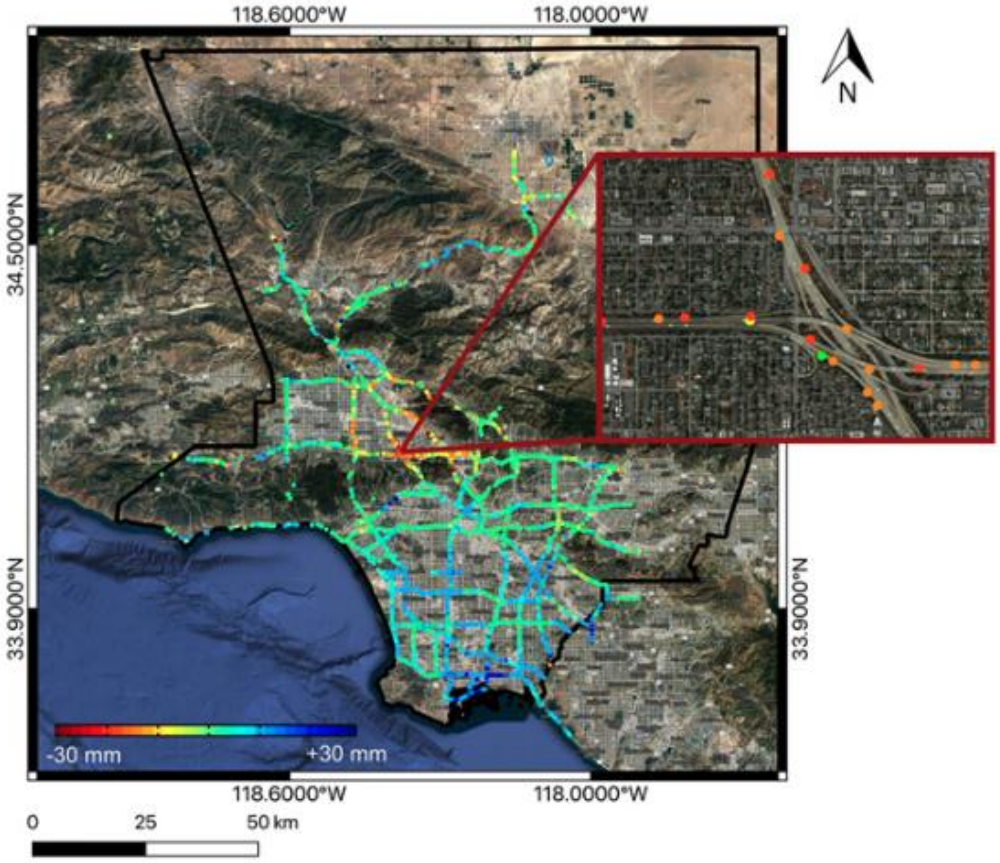

Figure 9. Cumulative displacement map of the Los Angeles highway and freeway network (Macchiarulo et al., 2022). Negative values indicate targets moving away from the satellite.

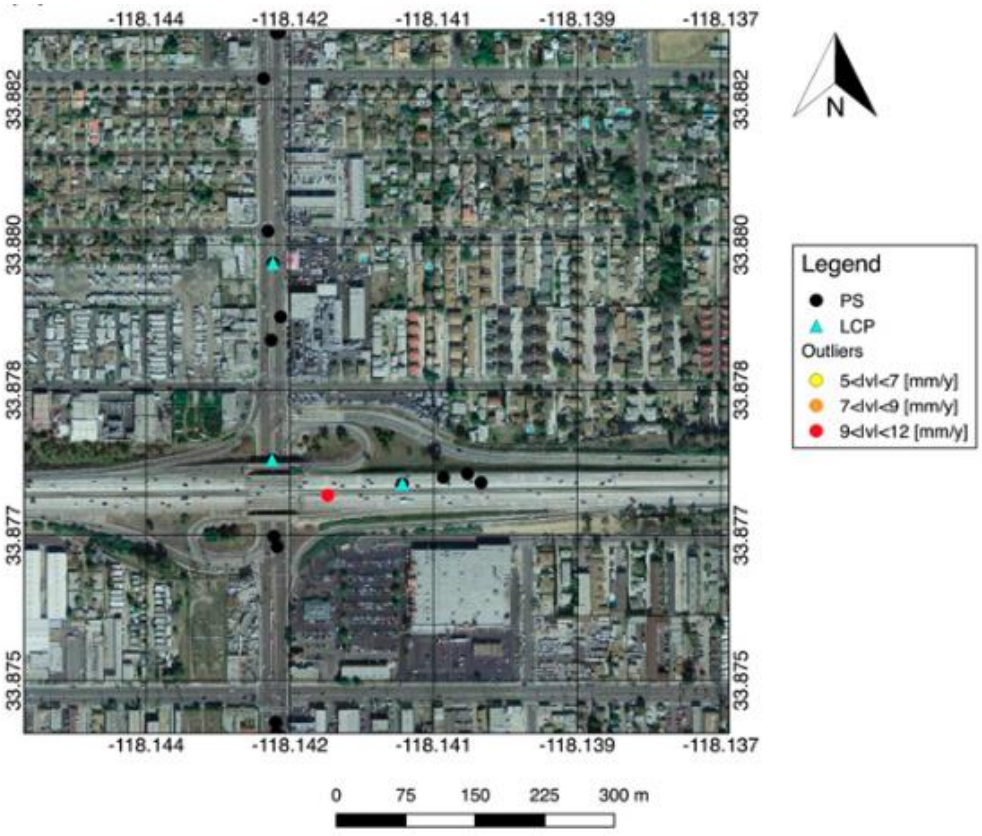

Figure 10. Los Angeles, map showing an example of outlier (in red) (Macchiarulo et al., 2022)

2.3 Light Detection and Ranging – LiDAR

Overview

Light Detection and Ranging LiDAR is a method that calculates the distance to a given object by measuring the time delay between an emitted laser beam and the reflected signal. The intensity of the reflection can also be monitored. LIDAR is an extremely fast, accurate, non-destructive technology with diverse processing options today. However, as with all types of fast emerging technology, users must be aware of their options and the limitations of each systems. It is essential that data is collected properly and processed in a way that preserves accuracy (Lacasse et al., 2022).

LiDAR technology can be utilized by two remote measurement techniques: Terrestrial Laser Scanning (TLS) and Airborne Laser Scanning (ALS). TLS (also referred to as ground-based LiDAR) is based on acquiring a point cloud of the terrain using the time-of-flight distance measurement of an infrared laser pulser (NGU, 2022). For common applications, a spatial resolution of one point every 5 to 15 cm is generally applied. Over the past decade, TLS has been used for geotechnical monitoring of tunnels (during construction and post construction; degradation), rock cuts and rockfall along linear infrastructure corridors, landslides, dams and building deformation. TLS has very high resolution and provides superior measurement precision and accuracy compared with airborne LiDAR and UAV applications. Figure 11 show, as an example, an integration of TLS with ground-based physical sensors in a full-scale field test of a cut slope at the Øysand test site in Norway (Shin et al., 2020). The ground-based LiDAR system (Figure 11e) was utilized to monitor the global deformations of the slope.

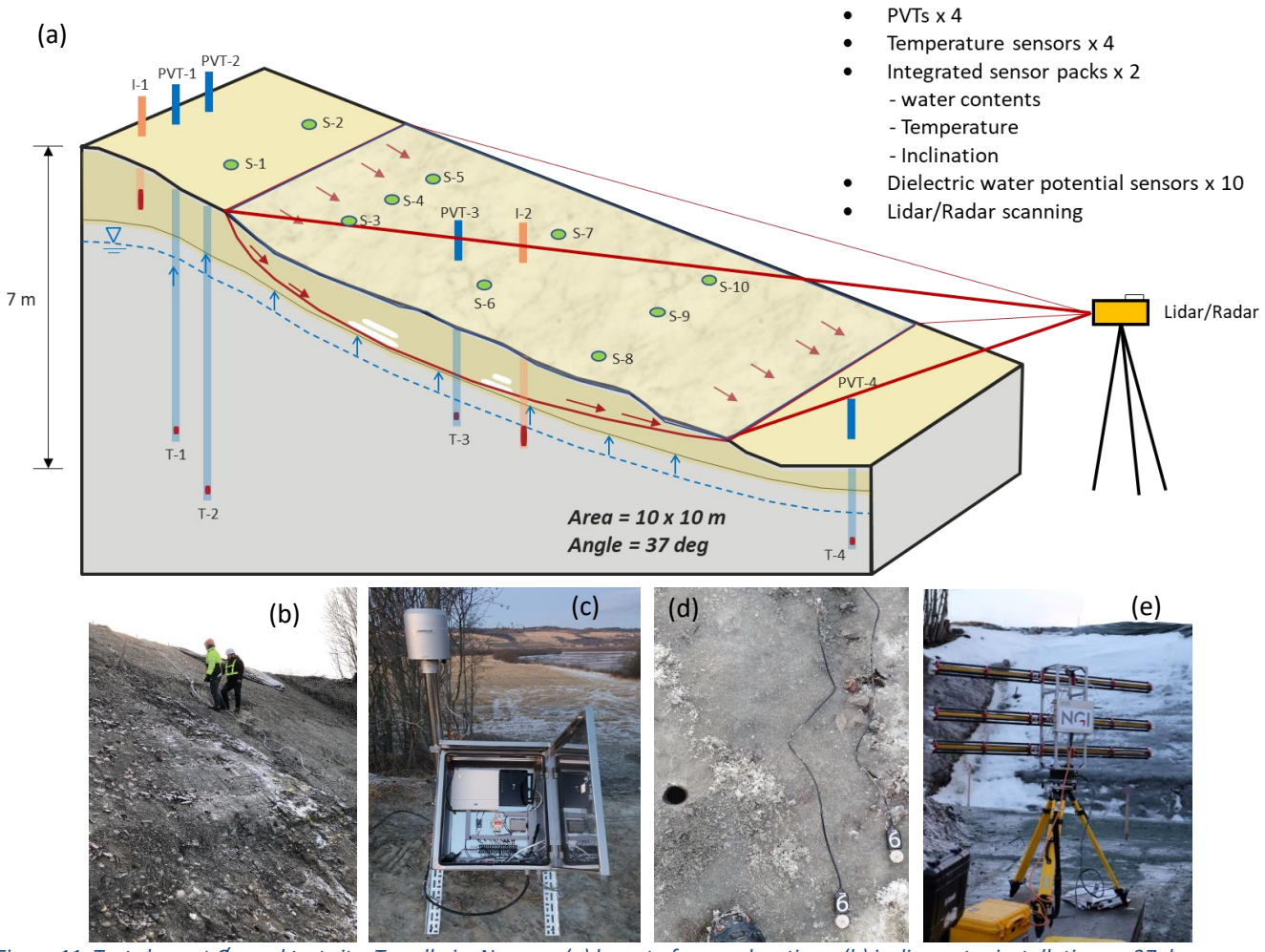

Figure 11. Test slope at Øysand test site, Trondheim Norway: (a) layout of sensor locations; (b) inclinometer installation on 37 degree man-made test slope; (c) data logger box at top of the slope; (d) MPS-6 sensors; (e) LiDAR system (Shin et al., 2020).

Similarly, ALS has also been used for monitoring of unstable slopes and settlement analysis in urban areas. Two types of system currently exist to capture airborne LIDAR data: a classical manned airborne and lightweight Unmanned Aerial Vehicle (commonly referred to as a drone) (Meade, 2021). Airborne LiDAR is capable of obtaining detailed measurements over a short timeframe for large areas/distances. Classical airborne surveys conducted from an airplane are usually less accurate, but they can cover up to 1000 km^2 in one flight. The accuracy depends on the flight height and the choice of sensors. On the other side, lightweight drone (or UAV) LiDAR systems will cover as much as the drone allows per flight, between 25 to 65 km per day. The UAV LiDAR can be more accurate than those carried by aircrafts, but airborne LiDAR can cover much larger area and less weather dependent (Meade, 2021).

Figure 12. Operating drone-based 3D mapping (Image: NGI)

Both TLS and ALS are still regarded as costly tools and therefore generally used only once site conditions have deteriorated. This poses a challenge for achieving optimal monitoring results since a baseline cannot be established.

Earlier study by Sutarto (2014) showed that LiDAR pulses bounced back from water surfaces such as in streams instead of the underlying ground surface. LiDAR pulses can also have problems penetrating though vegetation cover due to the returned signal being filtered out by vegetation. Dense vegetation cover and water reflection can still interfere with LiDAR measurement accuracy and skew the results (Meade, 2021).

Application of LiDAR to the investigation of potential geo-hazards

Partner: Norwegian Geotechnical Institute (NGI)

NGI's long-range terrestrial laser scanner (Optech Ilris LR) has been used to investigate rockfaces for potential geo-hazard issues, whereas the short-range scanner (Faro Focus 120) has been used to map internal structures such as tunnel walls. During data processing, LiDAR data was analysed with specialized software to automatically identify the most abundant sets of planes and give information about structural discontinuities. This enables a geologist to better assess rockslide or rockfall hazards. A development has been made at NGI to include fast algorithms and parallelization, facilitating the efficient computation of the minimum absolute distance between two LiDAR-acquired surfaces. For example, this tool offers a detailed, non-destructive way to find the actual thickness of a shotcrete layer.

A GigaPan robot (i.e. gigapixel panoramas, digital images with billions of pixels) has been used at NGI as supplement to LiDAR scans with high-resolution, automated panorama pictures. GigaPan is simple to use and capable of providing immediate results which have been proven to be beneficial in the post-processing of LiDAR data.

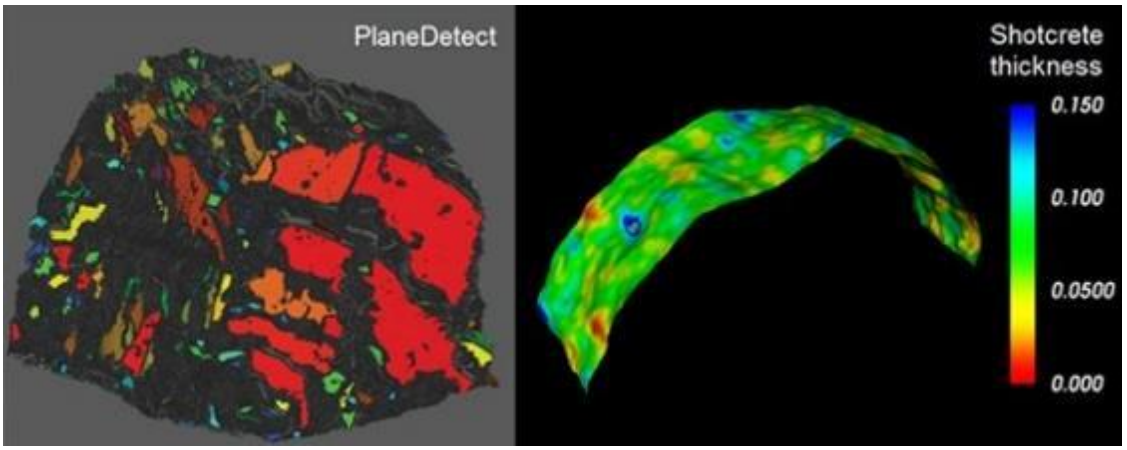

Figure 13. Planes are automatically detected and classified according to orientation (left) based on LiDAR-scan. The thickness of shotcrete layers (in meter) in tunnels can efficiently be calculated (right). (Image: NGI)

Figure 14. GigaPan imaging technology generates a panorama with extremely high resolution (Fedafjorden and Flekkefjord) to supplement LiDAR-data (Image: NGI)

3 Geophysical methods for subsurface imaging

Victor Hopman
Deltares, Netherlands

Stanislav Lenart
Slovenian National Building and Civil Engineering Institute, Slovenia

Ángel Tijera Carrión, Rubén Ruiz Bravo
CEDEX, Spain

Jean-Sebastien L'Heureux, Thi Minh Hue Le
Norwegian Geotechnical Institute, Norway

3.1 Background

Geo-engineering of critical infrastructure has in recent decades become open to exploring different advanced cross-disciplinary techniques for reducing risks during construction and maintenance. Among various technologies, geophysical techniques are increasingly used to monitor and characterize structures and underground condition. Compared with boreholes, which are traditionally used by geo-engineers, geophysical methods are advantageous in terms of their non-intrusive / non-destructive nature and their capability to provide spatially continuous information. The development of information technology has in addition accelerated the development of geophysical methods in the last decades (Setchell et al., 2016).

The most popular geophysical techniques utilized in monitoring / characterization rely on measurements of seismic vibration, electrical resistivity, electromagnetic properties, magnetic fields or radio pulses. Many of these techniques have been employed by partners in GEOLAB consortium in both laboratory and field research and development activities. This chapters present some applications of geophysical techniques deployed by the GEOLAB consortium partners.

3.2 Electrical Resistivity Tomography - ERT

Overview

Electrical Resistivity Tomography (ERT) is an advanced geoelectrical technique which is becoming more and more popular for both imaging and characterization of the sub-surfaces. ERT has been used for several decades in geophysical exploration and has gained popularity for geotechnical applications in the last 15-20 years. ERT can be used to measure the electrical conductivity in order to characterize the subsoil or to monitor an area continuously so that temporal changes are spotted. ERT data can be acquired with electrodes installed permanently or temporarily, and the data can be acquired relatively quickly with recent developments in automation of data acquisition.

ERT uses two current electrodes to inject a Direct Current (DC) into the ground and two potential electrodes to measure the potential difference (Figure 15). The apparent resistivity distribution of the

subsurface can be determined by injecting current and measuring potential using different combinations of electrodes, each sensitive to a certain part of the volume. The true resistivity distribution is then found by inversion of the data (Revil and Jardani, 2010). The DC electrical conductivity σ_0 (expressed in S/m) of a porous rock or soil is the reciprocal of the DC electrical resistivity ρ_0 (in Ohm·m), i.e., $\sigma_0 = 1/\rho_0$. Electrical conductivity represents the ease with which an electrical current is flowing through the Earth. An electrical current represents the flux of charge carriers through a given cross-sectional area. A water saturated rock or soil is, at least, a two-phase composite consisting of a solid mineral phase and pores, which are saturated by an electrolyte. Usually, most of the grains are not conductive and the conductivity is restricted to the pore water. In European countries such as the Netherlands, Norway where soft soils with high water content are widespread, the use of ERT to differentiate conductive soft soils from not conductive rock is possible.

A typical acquisition system for DC resistivity measurements is shown in Figure 15. It comprises a resistivity meter, a battery, a switching box, several cables, and electrodes. For each measurement, two current electrodes are used: one to inject the current into the subsurface or a sample and the other to retrieve the same amount of current from it. By convention, these electrodes are named A and B, respectively. The electrical field is measured with two other electrodes (M and N) called the potential electrodes. The current electrodes cannot be used at the same time to measure the associated drop of the electric potential in the Earth, due to the contact impedance across the electrodes, especially at low frequencies. The resistance R (in Ohm) measured across a cylindrical core sample of resistivity ρ (in Ohm m), length L, and cross section A is given by $R = \rho L/A = \rho / g$, where $g = A/L$ (in m) is called the geometric factor. For field acquisition, the geometric factor depends on the position of the electrodes as discussed below. The resistance is obtained by applying Ohm's law, $U = R I$, where U is the voltage (difference of potential) measured between M and N and I is the strength of the injected current.

The measurements represent the resistivity that the ground would have had if it were homogeneous. In most cases the subsoil is represented by an inhomogeneous earth. Therefore, in practice the measured apparent resistivity represents a weighted average of the true resistivity of the subsurface. This value cannot be used directly, and the true resistivity can only be found after further processing of the data. Inversion can be difficult due to processing aspects such as:

- Existence: there may be no model that exactly fits the data;
- Uniqueness: if exact solutions do exist, they may not be unique, even for an infinite number of exact data points; and
- Instability: the process of computing an inverse solution can be, and often is, extremely unstable in that a small change in measurement makes enormous change in the estimated model.

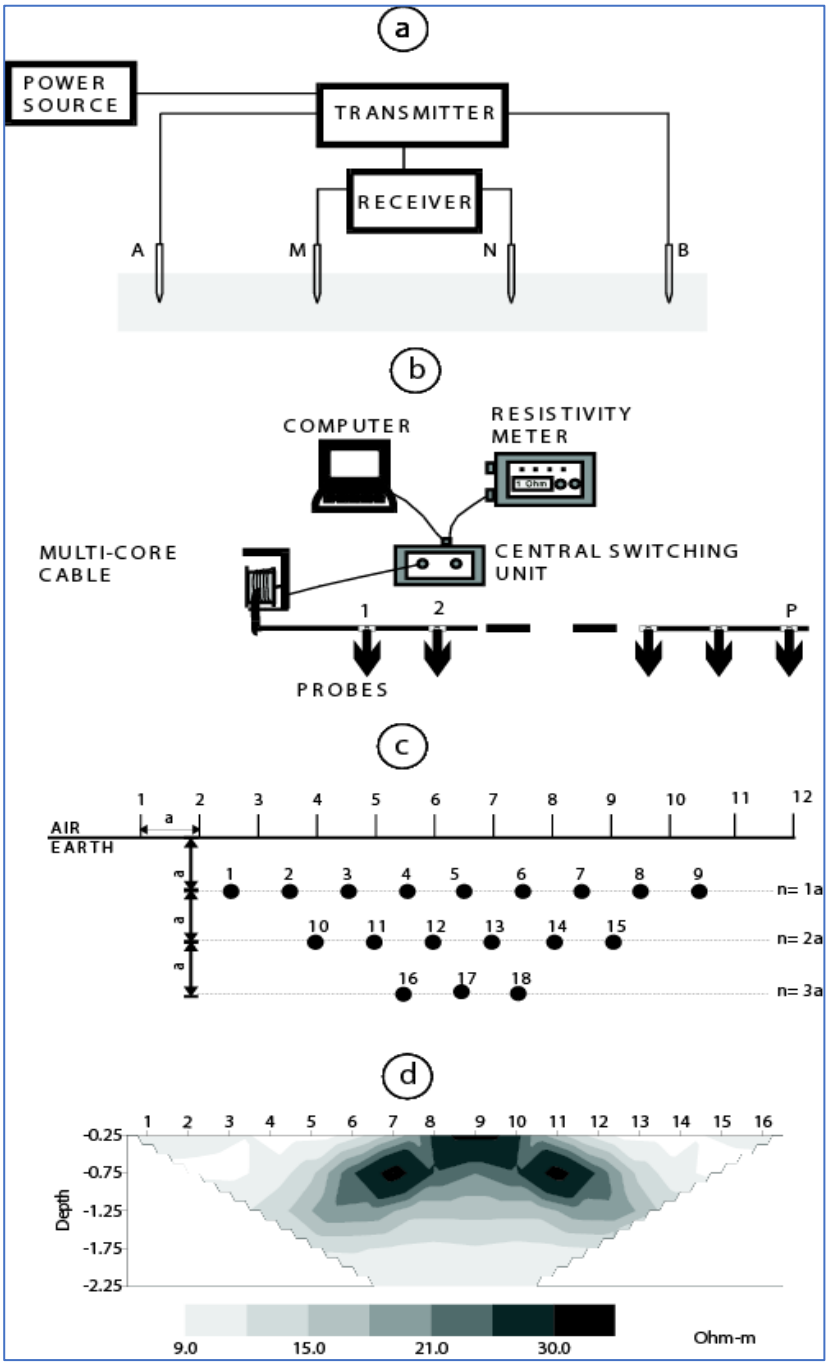

Figure 15. The principle of an ERT measurement: (a) basic measurement with 4 electrodes for a resistance measurement; (b) Principle system layout of a central switching computer-controlled resistance measurement: (c) collecting data by different combinations of electrodes (probes); and (d) data collect to process for a full 2D plane (Image: Deltares)

Application of ERT in the laboratory to the detection of a PE membrane

Partner: Deltares

Polyethylene (PE) membranes are used as groundwater barriers in infrastructure works in situations with high groundwater levels. In the Netherlands, the topography of the land is generally flat and groundwater levels are high. Tunnels, bridges and trenches are constructed at crossings of different means of transport such as roads, waterways and railways. In some cases, a PE membrane is applied to prevent groundwater leakage. When reconstruction or maintenance works are necessary, the position of the membrane in the subsurface needs to be known.

No existing method was available to detect the position of the membrane with high spatial resolution. The goal was to achieve a vertical accuracy of ~10 cm. One of the favourable properties of a PE membrane is that PE is an electrical insulator. The contrast in electrical resistivity between the membrane and the surrounding subsoil is high. Electrical Resistivity Tomography (ERT) therefore appears to be the suitable technique in this situation. However, classical Electrical Resistivity Tomography (ERT) employed from the surface does not have sufficient spatial resolution to locate the membrane (Figure 16). Modelling has shown that electrodes need to be closely spaced and within 1.5-2.0 m from the membrane. To this end, a prototype tool was developed by Deltares for the Ministry of Infrastructure/Rijkswaterstaat of the Netherlands. The tool needs to be pushed in the ground. Measurements are obtained while approaching the membrane. A prototype was tested in the laboratory at Deltares.

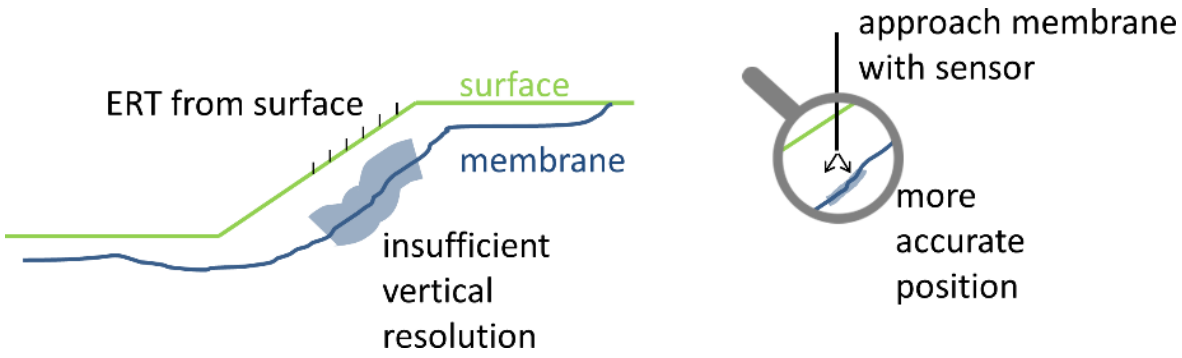

Figure 16. Sketch of ERT measurements from the surface versus penetrating tool (Image: Deltares)

The electrical insulation of the PE membrane causes the distortion of field lines. A modelling exercise was executed to investigate the best electrode configuration for a penetrating tool. The electrode configurations can be divided into those that are sensitive to a small volume near the tool ("close detection) and those that are sensitive to the presence of the membrane further away ('far detection").

Figure 17 shows two examples with varying distances between the electrodes. Electrode configurations with electrodes on the pole of the tool were also modelled. A combination of electrodes on the pole and on a "fork" at the end of the tool, with electrodes on the surface and/or on the tool is required to properly determine the resistivity distribution. The remote electrodes in the "far detection" configuration promote the detection of the membrane from a relatively large distance. The modelling was used to predict kernels, which were used during the inversion of the laboratory data.

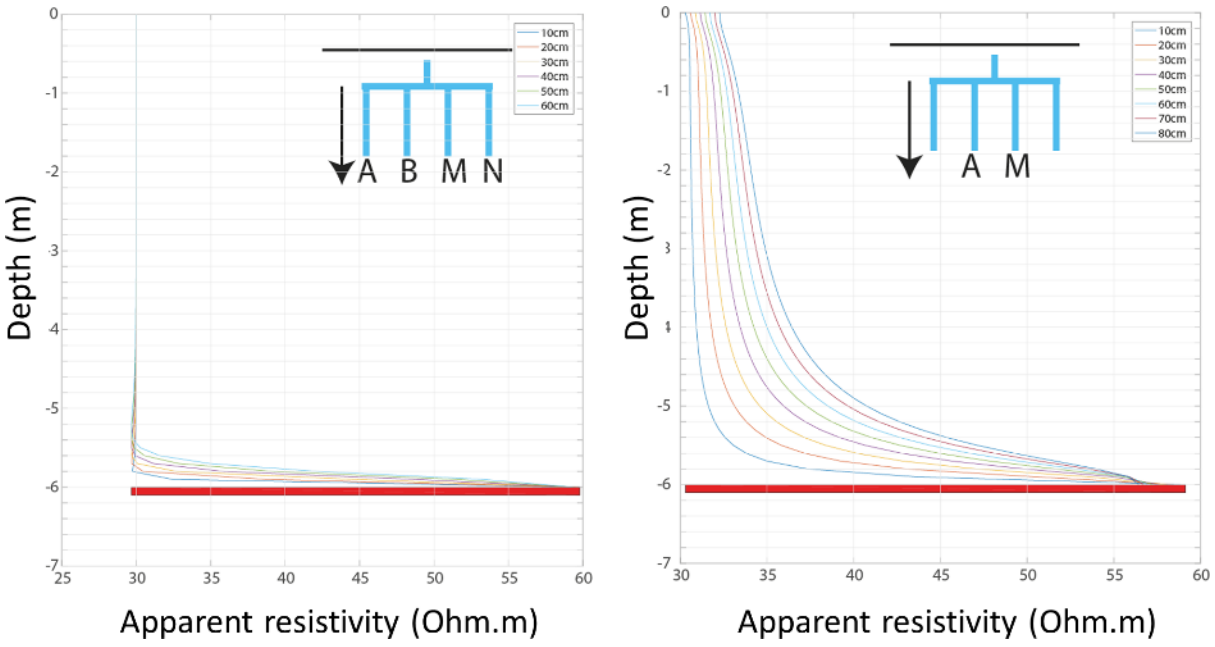

Figure 17. Examples of modelling results. Different lines indicate different distances between the electrodes on the tool. Left: configuration sensitive to "close" detection, with all electrodes on the tool. The membrane is only sensed when the tool is really close to the membrane. Right: configuration sensitive to "far" detection at a relatively large distance from the membrane, with current electrode B and potential electrode N at the surface at a large distance (remote electrodes). (Image: Deltares)

The modelling result was used in the design of the tool. Two prototypes were built for laboratory tests (Figure 18). A low-cost and simple wooden tool with electrodes for tests in a water tank and a robust coated metal tool for tests in a tank filled with sand and clay. The experiments were carried out in a PE tank of size 7 m x 3.5 m and a depth of 2.5 m. The experiments in the water tank allowed for easy variation of configuration and movement of the tool, because of the lack of friction. Moreover, the water tank provided a homogeneous medium. The experiments in the tank filled with sand or with sand and clay resembled field conditions. Because of the friction and the disturbance of the measurement, the experiments in the sand tank were performed only once.

Figure 19 (left) shows the setup of heterogeneous experiment with both sand and clay. The "close" detection configurations were used to calculate the background resistivity of the medium (Figure 19, centre). This background resistivity is required to correct the kernels for the effect of the membrane. The clay results in local decreases of the resistivity (Figure 19, right).

The measurements were inverted for the position of the membrane. Kernels were calculated using the background resistivity and various assumed positions of the foil for 8 selected configurations that were sensitive to the presence of the membrane. The inversion scheme is known as "compact source inversion", where the favourable model is enforced to have minimal area. The configurations are for electrodes on the fork of the tool, with different distances between the electrodes, and therefore representing a different size of the tool. The true position was found by minimising the difference between the measured data up to a certain distance from the membrane and the kernels. For configurations with a relatively narrow fork, the tool needed to be very close to the membrane (0.3 m) to determine the position with the required accuracy of 10 cm. For other configurations with a wider fork, the correct position of the membrane could be determined at a distance of 0.6 m even in the presence of clay. When the tool was further away from the membrane, however, the results show that

the membrane is not yet near the tool. It is therefore safe to approach the tool a bit closer without puncturing the membrane and repeat the measurement.

The laboratory tank had a limited size. Therefore, the remote electrodes could not be positioned truly remotely. Their benefit of distorting the field lines at a large distance from the membrane was therefore relatively small. It is expected that the placement of remote electrodes in the field will result in detecting the membrane from a larger distance. Nonetheless, the laboratory experiment provided useful information to catalyze development of a tool that can be used in the field in the future.

Figure 18. Left: prototype for experiments in water. Right: prototype for experiments in sand and clay. There are electrodes in the pole and on the two "forks" at the end of the pole. (Image: Deltares)

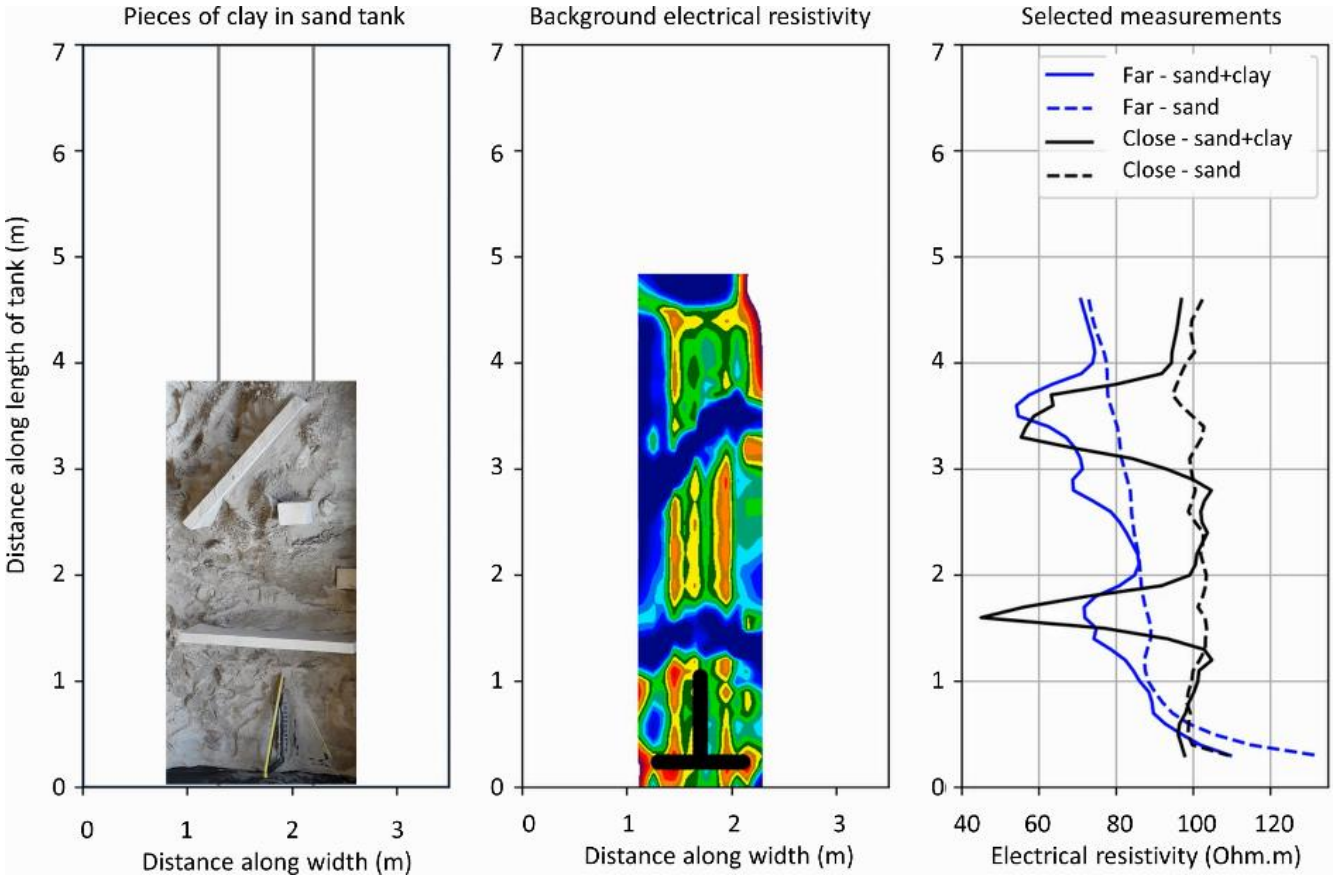

Figure 19. Left: layout of sheets of clay in a tank filled with sand. The membrane is located at the bottom of the plot at distance 0. Middle: background electrical resistivity recovered from measurements starting with the tool at the top of the figure and approaching the membrane. The position of the tool close to the membrane is indicated by the black inverted T. Clay shows up as low resistivity (in blue). Right: selected measurements for close detection (for background) and far detection (for membrane location). (Image: Deltares)

Application of field testing of ERT in the field for detecting potential quick clay

Partner: Norwegian Geotechnical Institute

Quick clay is characterised by complete collapse and liquid-like mobility when overloaded. Quick clay is found primarily in Norway and Sweden, but also exists in Finland, Russia, Canada and Alaska. Quick clay landslides, with their retrogression characteristics and extreme mobility, pose significant risk to human lives, infrastructure, property and surrounding ecosystems. Hence, the proper characterization of quick clay sites is essential for ensuring the safety and resilience of infrastructure in Norway and elsewhere in Europe.

Within GEOLAB, NGI supported two Transnational Access projects in 2022 (RELERT and QC-CEM) within which ERT methods were tested as a means for detecting potential quick clay areas. The ERT survey was conducted in June 2022 at the Tiller-Flotten quick clay site, managed by the NGI. The site is designed especially for field testing of innovative equipment, methods and technologies in real field condition closed to operational environment (L'Heureux et al., 2019). The site has been characterised in detailed with a number of rotary soundings, CPTU, samples and geophysical methods. A number of ERT profiles with different electrode configurations were carried out at the site to find an optimal configuration for detecting "leached" clay which is potentially quick.

Figure 20 shows the field work which were carried out by researchers from user groups (Luleå University) and NGI geophysicists.

Figure 20. Field study carried out in June 2022 at Tiller-Flotten quick clay site for Transnational Access project QC-CEM and RELERT (Photo: Olgert Gjuzi).

The results from ERT survey were compared with the data from geotechnical rotary soundings and laboratory samples from the same profiles. Figure 21 shows an example of a ERT profile at Tiller-Flotten. The ERT data indicates that the quick clay appears to fall in the region with electrical resistivity between 20 and 80 Ohmm based on comparison with rotary soundings. The results confirm previous studies in showing that ERT can be a useful technique for detection of potential quick clay pockets, however, the influence of local variation on ERT measurements needs to be investigated further.

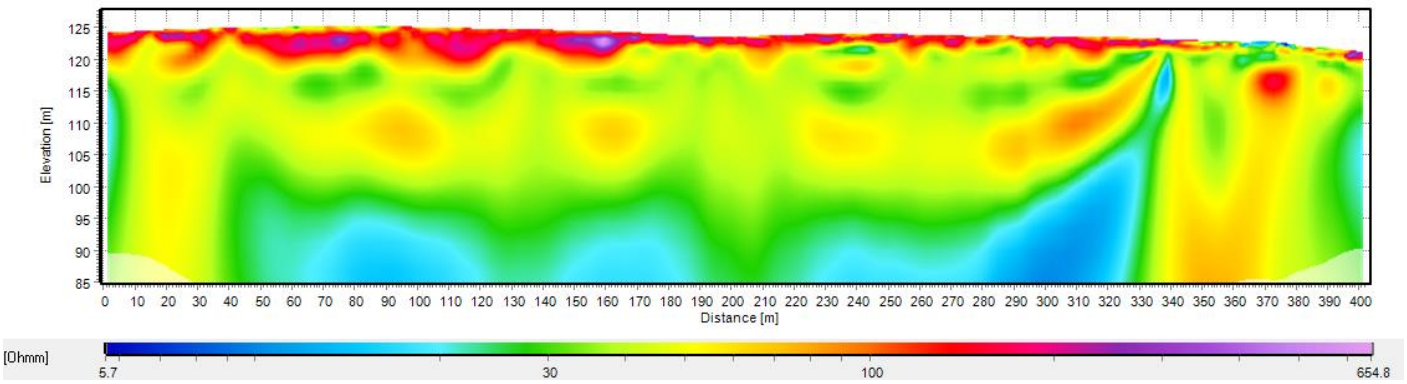

Figure 21. Example electrical resistivity measured with ERT for a profile at the Tiller-Flotten test site.

3.3 Seismic investigation

Overview

Seismic methods consist of measuring the response of the ground when mechanical waves, usually artificially generated, propagate through the ground. In most cases, the waves are generated by a device acting as a source, and sensors in contact with the ground (geophones or accelerometers) or water (using hydrophones) are used to record these waves.

The main objective of seismic techniques in geotechnical applications is to obtain the propagation velocities of waves traveling the ground. These waves can be of internal type (body waves: longitudinal or P-waves, and shear or S-waves), or surface type waves. Once the values of the propagation velocity of

longitudinal (v_P) and shear (v_S) waves are known, it is possible to calculate Poisson's ratio (ν). And if the density of the medium (ρ) can be calculated or estimated, it is immediate to obtain the dynamic stiffness moduli of the medium under study (shear stiffness modulus, *G*; and Young's modulus, *E*), as shown in equations (1), (2) and (3):

$$\nu = \frac{1}{2}\left[\frac{1 - 2\left(\frac{v_S}{v_P}\right)^2}{1 - \left(\frac{v_S}{v_P}\right)^2}\right] \quad (1)$$

$$G = \rho \cdot {v_S}^2 \quad (2)$$

$$E = 2(1 + \nu)\, G \quad (3)$$

Therefore, with these techniques, it is possible to know the distribution of the different materials that make up the ground and their mechanical properties.

In the above equations, it is observed that an increase in v_P and v_S implies an increase in stiffness. The propagation velocities of seismic waves are intrinsic characteristics of the medium through which they travel.

The following seismic techniques, performed from the surface, are widely used in geotechnical engineering applications:

- Seismic refraction; andAnalysis of Surface Waves.

These techniques are carried out from the surface, the ground is disturbed, usually by hammer impacts or falling masses, and a linear array of sensors is installed to pick up the generated waves, which are recorded on a seismograph or recording system for later analysis.

Seismic refraction allows the distribution of P-wave propagation velocities with depth to be obtained quickly and easily. Although less common, it is also possible to obtain S-wave propagation velocities using appropriate sensors and sources. A ground profile is obtained in which the different layers correspond to materials with different wave propagation velocities. A schematic sequence with different processes of the method is presented in Figure 22.

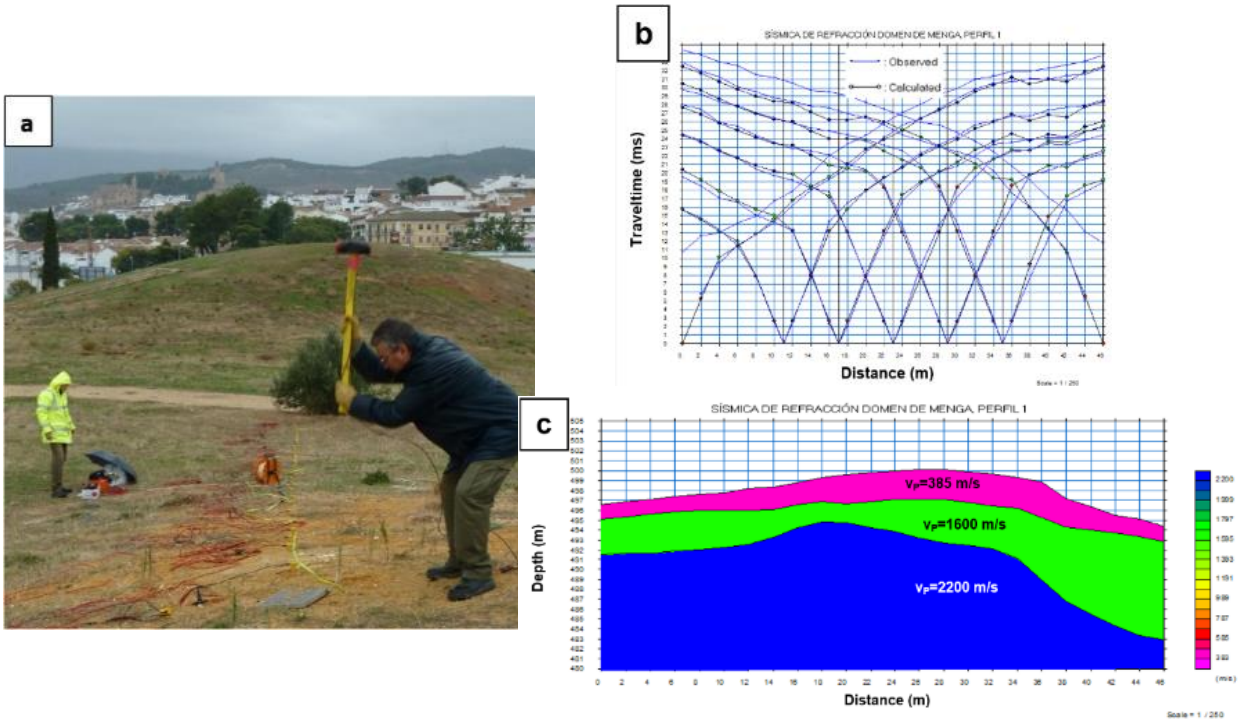

Figure 22. Schematic sequence with different processes of the method. (a) Data acquisition. (b) Interpretation of arrival times and layer assignments. (c) Layer models with different v_p (Image: CEDEX)

Among the most frequent applications are:

- Foundation and "rippability" studies
- Mapping of rock level, water table, faults, etc.

Surface waves analysis techniques study a type of waves that travel at the interface between the ground and the air. These waves are generated and propagated from the ground surface and from their analysis, using an appropriate inversion algorithm, the distribution profile with depth of shear (S) waves can be determined.

There are several surface wave analysis techniques, the most common in geotechnical applications are the following:

- Spectral Analysis of Surfaces Waves (SASW);
- Multichannel Analysis of Surfaces Waves (MASW); and
- Passive seismic microtremor analysis (ReMi, Refraction Microtremor).

Figure 23 shows two photographs of the data acquisition process in a MASW campaign and Figure 24 shows a photograph of some of the sensors and sources used in the SASW method, as well as a sketch of the test procedure.

Figure 23. MASW test data acquisition. (a) Source and sensors array. (b) Sensors array. (Image: CEDEX)

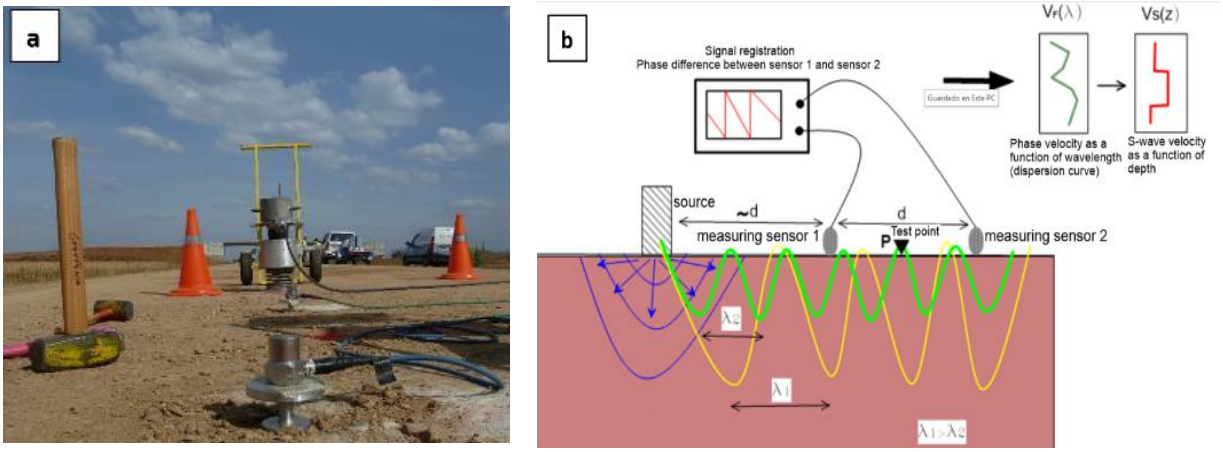

Figure 24. MASW method. (a) Photograph of some of the sensors and sources commonly used. (b) Sketch of the test procedure: The wave phase shift between two sensors is measured to obtain the ground dispersion curve and from this an equivalent v_S profile is generated. (Image: CEDEX)

The most frequent applications include:

- Monitoring of embankments, rockfills, landfills, earth dams;
- Foundation studies;
- Dynamic behaviour of soils;
- Characterization of the subsoil in kilometric studies in linear works; and
- Studies carried out on asphalted sites.

Soil characterisation in the RIVAS project

Partner: CEDEX

Ground vibrations caused by the trains passing by are a major environmental problem affecting many European citizens living or working near railway infrastructure. The European Union, within the 7th Research Framework Programme, funded the Rail Induced Vibration Abatement Solutions (RIVAS) project, which aimed to provide tools and methods to reduce vibrations below the annoyance threshold. This project involved railway operators, infrastructure managers, infrastructure and rolling stock manufacturers, and construction companies.

CEDEX participated in the working group that oversaw evaluating mitigation measures based on sub-grade improvement and ground barriers within the railway infrastructure. A series of experimental sites were chosen where, barriers were built in the vibration transmission path. It was necessary to characterise the ground and modelling its behaviour under the vibrations produced by the railway, to choose the appropriate barrier. The chosen techniques to characterise the ground were mainly seismic methods.

The test location was located near El Realengo, southeast of Spain, along the conventional railway line between Murcia and Alicante. There, two sites were chosen, the test site in which the barrier would be constructed and a reference site with the same geotechnical properties that will be used to provide context for the results at the test site. A high–speed railway line from Madrid to Levante was under construction adjacent to the conventional line at the time the study was carried out. Therefore, recent geotechnical information was available to the study. Despite that, a series of seismic measurement campaigns were performed to determine the dynamic characteristics of the ground. Specifically, the following tests were carried out:

- Spectral analysis of surface waves tests (SASW) (4 of);
- Seismic refraction surveys (SR) (4 of);
- Downhole piezocone seismic tests (SCPTU) (2 of); and
- Free field transfer functions tests and 2 track-field transfer function tests (2 of).

Figure 25 shows the setup and testing process. The SASW and refraction seismic tests provided v_P and v_S ground profiles that were used to model the most effective barrier for vibration reduction. The water table was found by seismic refraction at 1.5 m. The SCPT tests were used to check the values, "calibrate", of the central points of the profiles obtained from the SASW and SR tests, carried out from the surface. Transfer function tests were performed with the same sensors and sources used for the SASW test, and they were useful for testing the spatial damping ratio of vibrations propagating through the ground.

The ground profile provided by the seismic methods (presented in Table 1) was fed into different numerical models and finally, it was decided that a jet grouting wall (Figure 26) with a width of 1m, and a depth of 7.5m would be constructed. This meant a reduction in the depth of the screen of 2.5m with respect to the initial estimations made from the geotechnical information prior to the seismic tests.

Figure 25. Seismic refraction (left), SASW (center), and free field transfer function (right)(Image: CEDEX)

Table 1. Dynamic soil characteristics at the site in El Realengo. h is layer thickness, v_S and v_P are propagation velocities of S and P waves respectively, ßS and ßP are the spatial damping ratio for each kind of wave, and v is the Poisson´s ratio.

Layer	h [m]	v_S [m/s]	v_P [m/s]	β_s [-]	β_p [-]	ρ [kg/m^3]	ν [-]
1	0.30	270	560	0.123	0.123	1800	0.35
2	1.20	150	470	0.112	0.112	1750	0.44
3	8.50	150	1560	0.014	0.014	1750	0.49
4	10.00	475	1560	0.010	0.010	1900	0.45
5	∞	550	2030	0.010	0.010	1900	0.45

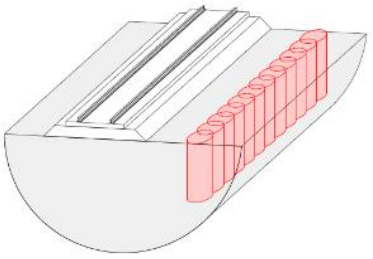

Figure 26. Sketch of the stiff wave barrier consisting of overlapping jet grouting columns. (Image: CEDEX)

To check the effectiveness of the barrier, ground vibrations induced by trains passing by were measured at the site and at the reference site before and after the construction of the barrier. That allowed for the experimental evaluation of the mitigation performance, demonstrating that the jet grouting wall was very effective in solving the vibration problems.

Full project information can be found on the website of the International Union of Railways, UIC[1] In addition, details of this work were published in 2015 (Coulier et al., 2015) .

[1] https://uic.org/projects/article/rivas

Characterisation of marine soils and landfills in port infrastructures

Partner: CEDEX

In collaboration with Puertos del Estado (the Spanish state-owned Port Agency) , the Geotechnical Laboratory of CEDEX carried out a three-year research work focused on characterizing marine soils and landfills using a variety of geophysical methods. An accurate in situ characterisation of these usually soft materials is essential to predict their performance under static and cyclic loading and to generate time evolution models. The goal of the study was to determine which combination of methods is most suitable, which was achieved via two phases of research:The first phase, which is the core of the research work, focussed on comparing the results obtained in a series of measurement campaigns carried out in the Port of Cadiz, with a ground model that was known a-priori. This served as a check on the suitability of the different techniques and facilitated the development of a working methodology that could be deployed on future geophysical characterisation projects.

The second phase consisted of the application and validation of the selected methods to study the foundation of a maritime station to be built on port reclamation land that has been in service for several years in the Port of Ibiza. At this site, one of the main objectives was to locate the bedrock on which the piles for the foundations of the facility were to rest.

The following seismic methods were applied: PS suspension logging, Down-Hole, SASW, and MASW. In addition to the seismic methods, an electromagnetic probe and a spectral gamma probe were used. Figure 27 shows some photographs of the surface wave tests carried out at both sites.

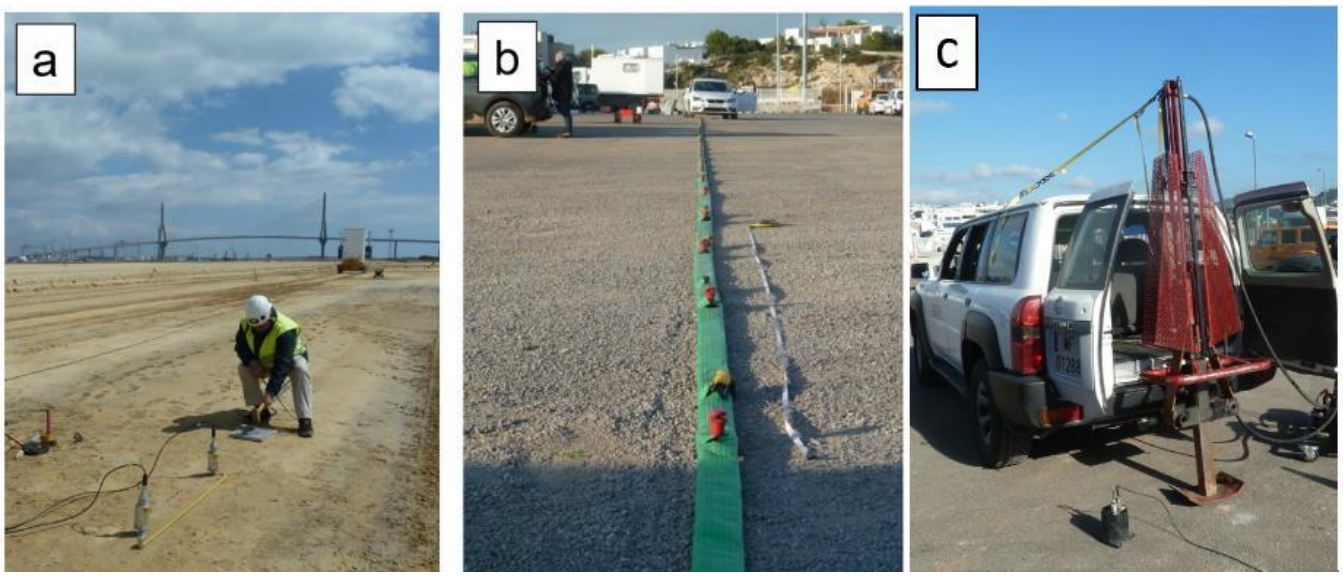

Figure 27. Surface wave tests: (a) in the foreground is the execution of a SASW test in Cadiz for a nearby sensor separation, in the background is the impact deflectometer used as a seismic source for large sensor separations; (b) seismic line used in one of the MASW tests performed in Ibiza; and (c) seismic source used in Ibiza. (Image: CEDEX)

In the first phase, a good correlation between surface wave methods and borehole seismic methods was observed, especially with PS suspension logging. The combination of surface and borehole seismic methods enhances the results provided by each seismic technique separately, combining the accuracy of borehole measurements with the extrapolation of results to large areas of land such as port esplanades.

In the second phase in Ibiza, excellent correlation between the SASW, MASW, and PS logging tests was again demonstrated. Figure 28 shows the results of these tests in the vicinity of two boreholes drilled at two points on the surface of the port esplanade. Due to the rapid execution, the MASW method was used to obtain a continuous surface of the bedrock substratum, which was finally located at an average depth of 17.5 m.

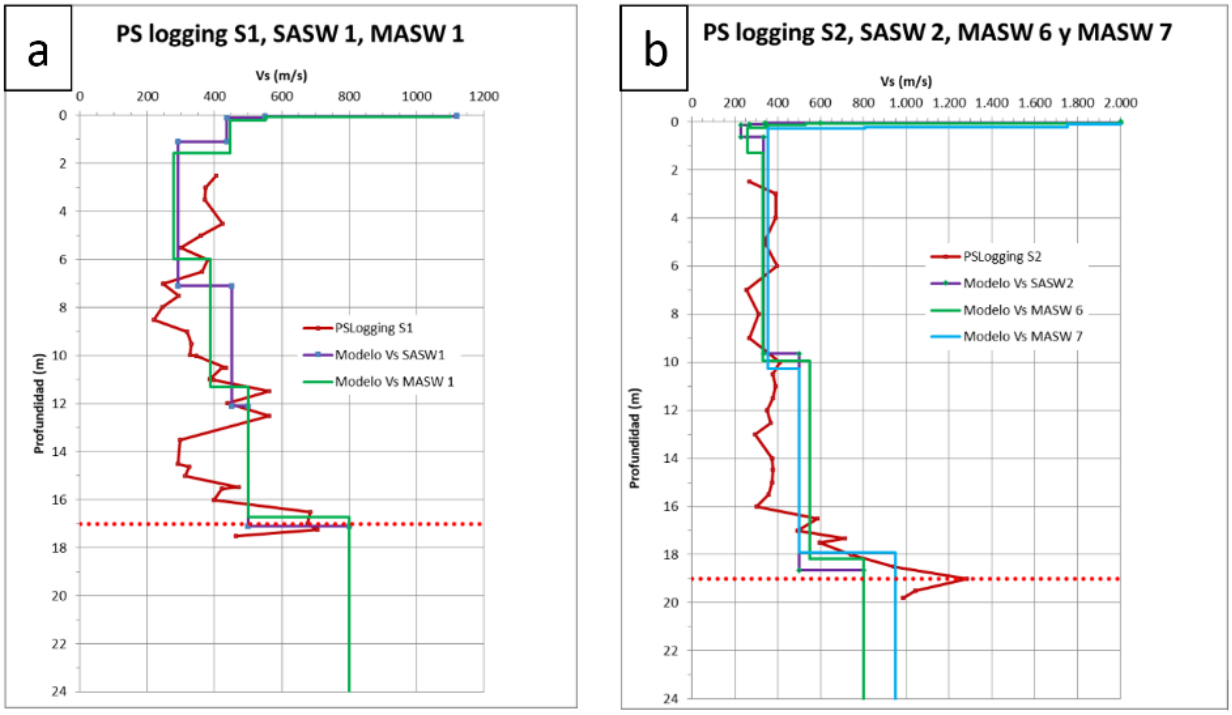

Figure 28. Shear wave propagation velocities were obtained with the PS logging probe in boreholes S1 (a) and S2 (b) and with the SASW and MASW tests closest to them. The stiffer, high-velocity material layer is marked with a red line. (Image: CEDEX)

The results of the first phase were presented in Tijera et al. (2019) and the results of the full research were published in Tijera et al. (2020).

3.4 Ground Penetrating Radar - GPR

Overview

A Ground Penetrating Radar (GPR) antenna consists of a transmitter and receiver and transmits an electromagnetic pulse of radio frequency into the medium. Typical GPR frequencies range between 100 MHz and 3 GHz. When the transmitted wave reaches an interface of differing material properties, part of the energy is reflected while the remaining energy continues its passage beyond the interface. The radar system will measure the time elapsed between wave transmission from the transmitter and reflections back to the receiver as well as the reflection strength. Figure 29 illustrates how pulses travel from transmitter in the medium to the receiver in an air-coupled GRP. It is common to conduct GRP with ground-coupled antenna. This is repeated at specified intervals while the antenna moves along the measurement line and the output (scans) are displayed consecutively in order to produce a continuous profile of the changes in material properties (reflections) in the medium (Figure 3).

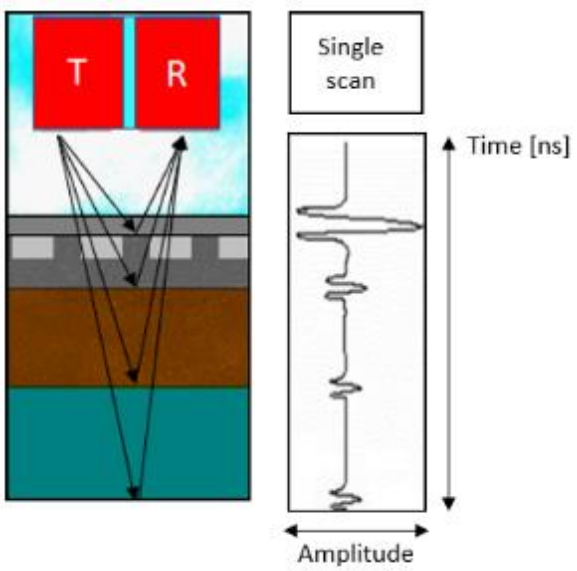

Figure 29. GPR principle (air launch). Electromagnetic wave is transmitted to the medium from the transmitter (T) and the receiver (R) records reflected signal travel time and amplitude. (Image: ZAG)

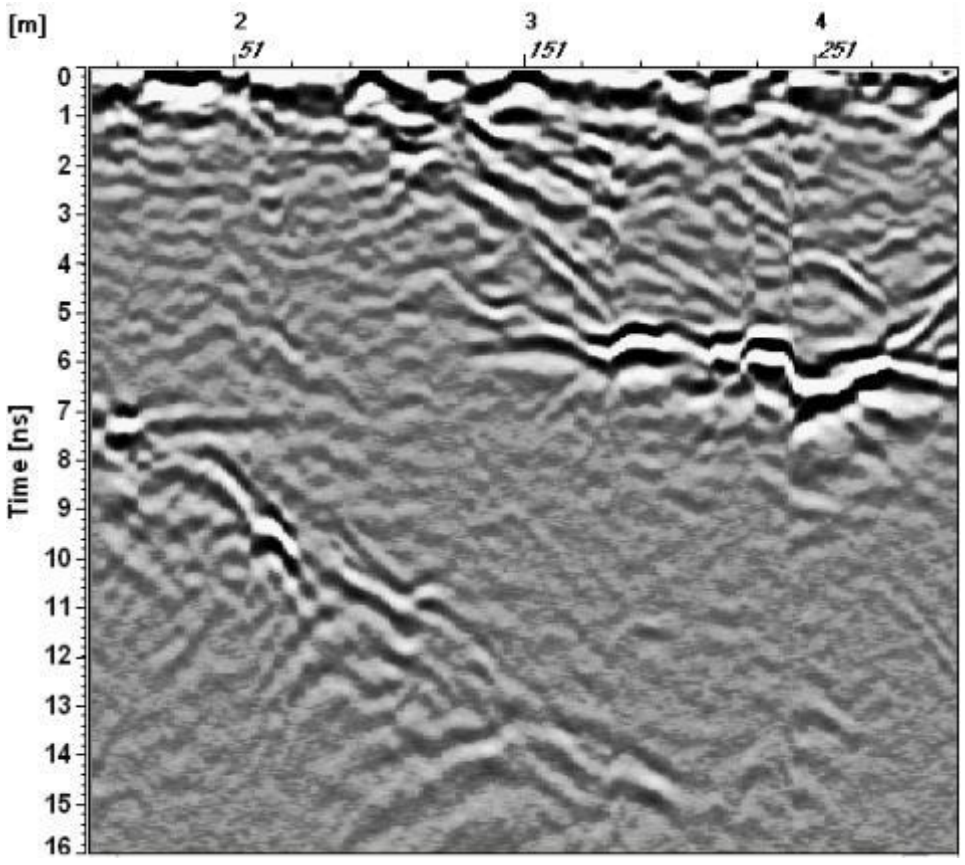

Figure 30. Example of longitudinal GPR profile from tunnel wall constructed from individual scans (Modified from Heikkinen and Kantia (2011)).

The wave velocity and reflection amplitude are affected by the dielectric permittivity, electrical conductivity (or resistivity) and magnetic susceptibility of the medium. In cases where the medium is a rock or mineral based material, the properties vary according to rock type, presence of conductive minerals, presence of porosity or fracturing, and the alteration and mineralogy of fracture fillings.

The signal wavelength or antenna frequency affects the ability of the system to identify objects of different sizes and different depths. For example, high frequency antennas have a better resolution of smaller particle sizes, but a shallow penetration depth, while low frequency antennas have a coarser resolution, but penetrate deeper into the medium. The degree of saturation with water, the salinity of water, and variations in porosity or fracturing intensity will also affect the net propagation of radar waves. The increase of water content in the medium will increase dielectric permittivity (and decrease wave velocity) as well as decrease resistivity (increase wave attenuation).

Ground penetrating radar (GPR) is widely used in road and railway maintenance and planning, particularly for structural condition monitoring, structure thickness assessment, and root cause identification of subsurface defects at both project and network levels (Silvast et al., 2013a, Silvast et al., 2013b). In this regard, GPR has been used in applications including: determining structures layer thickness, evaluating unbound materials quality, calculating moisture condition in structures, and identifying subgrade soil types. GPR is also suitable for mapping soil material thickness or stratification in soil material or snow if the depths are not large and the groundwater is not saline (which provides high conductivity). In addition, GPR can be used to locate various objects in the ground (e.g. pipes, large objects, cavities, rebars).

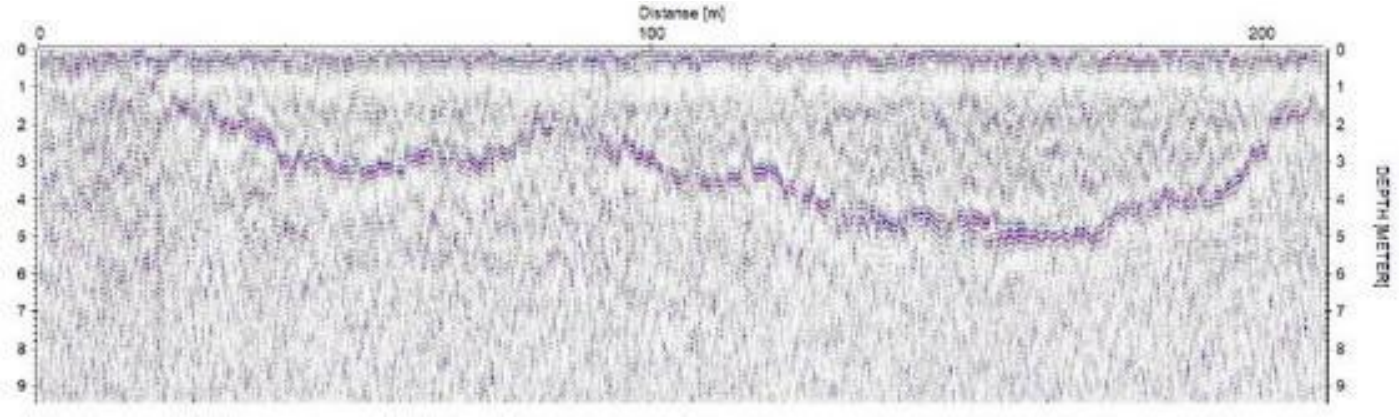

Figure 31. Radar diagram from a swamp area in southern Norway. Rocks were observed at each end of the profile (granitic gneiss), and the reflector visible through the profile is interpreted as the transition to rock / solid masses. The transmission speed of the soil materials is estimated on the basis of the conductivity and permittivity of the swamp material. (Image: NGI)

Application of GPR to the inspection of Cassia Monte Mario railway tunnel

Partner: Slovenian National Building and Civil Engineering Institute (ZAG)

Tunnel inspections must be carefully planned in order to keep tunnels open during inspection or to minimize tunnel closures. Visual inspection is typically the primary method used, however, wit is difficult to accurately and objectively analyse the condition of tunnel linings from visual inspection alone. Non-destructive testing methods like ground penetrating radar (GPR), laser scanner, and thermal imaging are methods for quickly evaluating rail tunnel linings on a mobile platform. Other common but stationary methods for NDT tunnel lining measurements are ultrasonic tomography, ultrasonic echo, ultrasonic surface wave analysis, and impact echo methods (Wimsatt et al., 2013).

There are significant benefits to using GPR in tunnel surveys. Detection of anomalies beyond the wall surface such as moisture defects, air-voids, and delamination can be examined through GPR signal

analysis. The lining thickness itself may be interpreted from the GPR data and depending on the materials used, anomalies in the underlying bedrock can potentially be investigated. There are also disadvantages to this technique. For example, steel fibres in a concrete lining cause interference in the GPR data, which can decrease the quality of the collected data (Silvast et al., 2019).

GPR technologies have been tested and used in several tunnel projects, however, they are not yet utilized to their fullest potential (White et al., 2014, Wimsatt et al., 2013, Zan et al., 2016). Comparison of different GPR technologies for road tunnel lining measurements, augmented with thermal imaging techniques, are presented by Wimsatt et al. (2013) and shown in Table 1. Figure 32 presents an example of measurement equipment in a point cloud tunnel environment. A laser scanner was used in addition in this case to detect surface defects and to acquire results in point clouds (Silvast et al., 2019).

Table 2. Comparison of different non-destructive testing methods for tunnel wall lining measurements (Modified from Wimsatt et al. (2013).

Method	Accuracy	Detection depth	Deterioration mechanisms detected	Tunnel lining type	Other info
Air-coupled GPR	Locates defects within 30 cm of its actual location	Does not measure depth but indicates areas of high moisture or low density (high air voids). Such areas may represent problems within or behind the tunnel lining.	Tile debonding, delamination, air-filled voids, water-filled voids, moisture intrusion	Concrete, tile lined concrete, and shotcrete	Scanning tool that can indicate where to conduct testing with in-depth devices.
Ground-coupled GPR	Can determine defect depth within 10% of the actual depth without reference cores 5% if cores are available.	Can possibly detect defects at any depth within or immediately behind tunnel linings. However, specimen testing indicates it cannot locate <0.3m2 voids in steel plates behind tunnel linings.	Delamination air-filled void water-filled voids, moisture intrusion	Concrete, tile lined concrete, and shotcrete	Experienced personnel are needed to interpret defect locations and depths from the GPR profiles.
Thermography / thermal imaging	Locates defects within 30 cm of its actual location	Does not measure depth, but indicates areas of high moisture or low density (high air voids). Such areas may represent problems within or behind the tunnel lining.	Tile debonding, delamination, air-filled voids, water-filled voids, moisture intrusion	Concrete, tile lined concrete, and shotcrete	Scanning tool that can indicate where to conduct testing with in-depth devices.

Figure 32. 3D GPR and thermal camera survey illustration in point cloud model from 2D laser scanner (Silvast et al., 2019).

The Cassia Monte Mario tunnel is located between the chainage km 2+600 and km 7+175 of railway Roma San Pietro - Vigna Clara, which was commissioned in 1990. The tunnel has a total length of 4,575 meters. The original constitution of the lining varies along the tunnel length alternating brick or stone masonry and concrete.

The tunnel was surveyed in the scope of the Assets4Rail[2] project, which was focussed onmapping problem locations in railway tunnels in 2021 (Silvast et al., 2021). GPR measurements were performed with a mobile platform to maximize the amount of collected data and minimize the tunnel closure time. For tunnel wall lining measurements, a special vertical antenna setup was required (Figure 33). The GPR used in this project was Geoscope MK IV + DX1821, which is a 1.8 meter wide, 21-channel step-frequency radar. The manufacturer is 3D-radar AS from Norway. The GPR antenna was attached to the shovel of a small railway excavator. The excavator was attached to a flatcar and the shovel was on or above the flatcar with the GPR antenna hanging from it outside the vehicle. Measurement equipment was installed on a railway vehicle, which consisted of an excavator and a flatcar.

[2] http://www.assets4rail.eu/

Figure 33. The GPR antenna DX1821 from 3D-radar attached to a shovel of an excavator on the flatcar (Silvast et al., 2021).

In this project Rail Doctor® software v. 3.5 from Loram Finland was used for data analysis. This software enables the user to simultaneously view, process, interpret and analyse multiple datasets that use the same co-ordinates, e.g., 3D GPR data from different antennas, digital video, structural databases and other reference measurements (Silvast et al., 2021). This kind of data combination allows the user to conduct an integrated analysis of all the available datasets on a single screen. An example of the GPR data view in Rail Doctor® can be seen inFigure 34. The upper grayscale image shows a profile slice of GPR data in depth at a height of 4.125 meters, while the lower image is a surface map of GPR signal amplitude from the tunnel wall surface in approximately 6 centimetres.

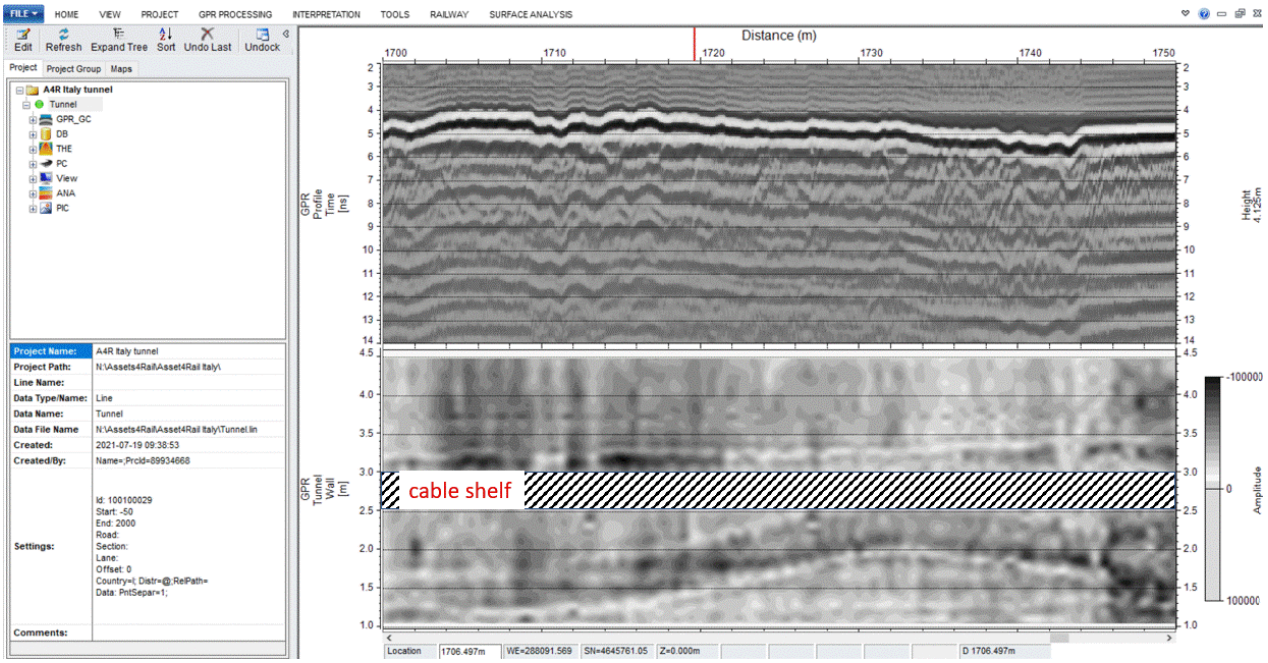

Figure 34. An example of GPR data in Rail Doctor® view (Silvast et al., 2021)

3.5 Electromagnetic survey – EM

Overview

An electromagnetic survey (EM) is based on the response of the ground to the propagation of electromagnetic fields composed of an alternating electrical intensity and magnetizing force (Haldar, 2018). The principles for electromagnetic survey are explained in detail by Haldar (2018) and illustrated conceptually in Figure 35. EM is commonly used in mineral explorations. In recent years, EM has been increasingly used for ground characterization in geotechnical engineering applications such as the identification of soil types, bedrock depth, and hazardous rocks such as alum shale and weakness zones (EMerald Geomodelling, 2022).

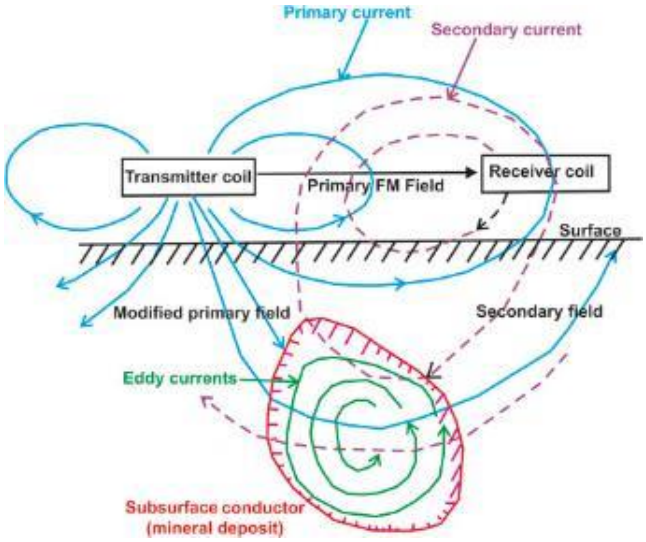

Figure 35. Conceptual diagram of electromagnetic induction processing system generating eddy currents in subsurface conductive mass (adapted from Haldar (2018))

EM survey can be conducted by both air-borne/drone-borne or ground and water-based devices. Figure 36 shows a ground investigation conducted with EM survey with SMARTx4 to test its capability to detect potential quick clay at the Tiller-Flotten test site managed by the NGI.

Figure 36. Equipment and ground investigation with ground-based EM survey conducted in June 2022 at the Tiller-Flotten test site. The research is within GEOLAB- Transnational Access project QC-CEM with user group from Luleå University (Photo: Olgert Gjuzi)

Airborne electromagnetic (AEM) surveying originated in the 1930's and has been internationally used for mining, geological mapping and groundwater applications (saltwater intrusion) since the 1980's. AEM data are collected by transmitting an electromagnetic signal from a system attached to an airplane or a helicopter, see Figure 37 (Pfaffhuber, 2014). The signal induces eddy currents in the ground which are detected by receiver coils towed below and behind the aircraft. AEM techniques can detect variations in the conductivity of the ground to a depth of several hundred meters, depending on the acquisition system and the site's geology. AEM surveys require complex processing to allow interpretation and, therefore, are usually designed to detect particular subsurface targets which are based on a perceived conductivity contrast (Geoscience Australia, 2022) such as provided by the presence of a substantial clay-rich layer, ground-water table or bedrocks.

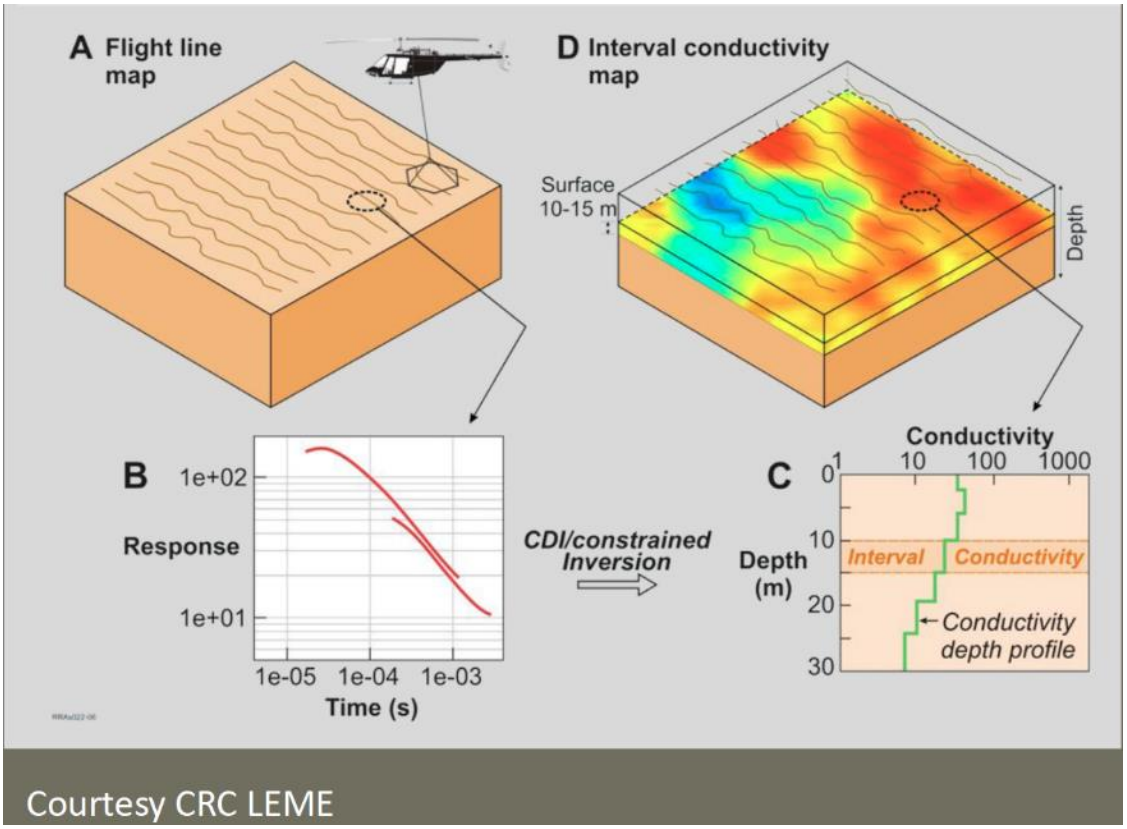

Figure 37. Different stages in AEM survey (adapted from Pfaffhuber (2014))

In the past decade drones have become increasingly available and affordable for civil applications, including the mapping and monitoring of the earth surface with geophysical sensors. The drone-borne electromagnetic system (DR-EM) has the ability to fly above inaccessible areas and surface water. Compared to air-borne electromagnetic surveys, the spatial resolution is much higher which allows for very detailed 3D mapping of subsurface targets and the costs are, certainly for small study areas, relatively low. Repeated drone-borne electromagnetic (DR-EM) surveys allow for low-cost monitoring of local changes in a target area.

Air-bone electromagnetics (AEM) system applied to road and railway projects

Partner: Norwegian Geotechnical Institute (NGI)

Large critical infrastructure projects such as roads and railways can be very challenging for geotechnical engineers to design, especially when they cross complex and varying ground conditions. Traditionally, site investigations for such projects included a combination of geotechnical soundings and boreholes, followed by geotechnical laboratory testing to determine soil properties. These methods are well proven, but time consuming, costly and only give local information on the ground conditions that must be interpolated between The resulting uncertainty when dealing with subsurface variability leads to unnecessarily expensive and less sustainable infrastructure design due to the need to conservatively manage risk.

Over the last decade, geotechnical researchers and practitioners, including NGI, has been seeking innovative solutions and new technology that can make site investigations more effective by saving time and reducing cost through AEM. NGI, through Emerald Geomodelling[3], hasapplied outcomes from research and development activities into AEM to provide the missing link between complex geophysical data and sparse geotechnical data in large infrastructure projects, particularly roads and railways.

AEM utilizes electrical conductivity as a proxy to identify soil type, depth to bedrock, hazardous rock type such as black shale that produces radon and major weakness zones (EMerald Geomodelling, 2022). Figure 38 shows the principle, typical setup for geo-scanning by AEM in the field.

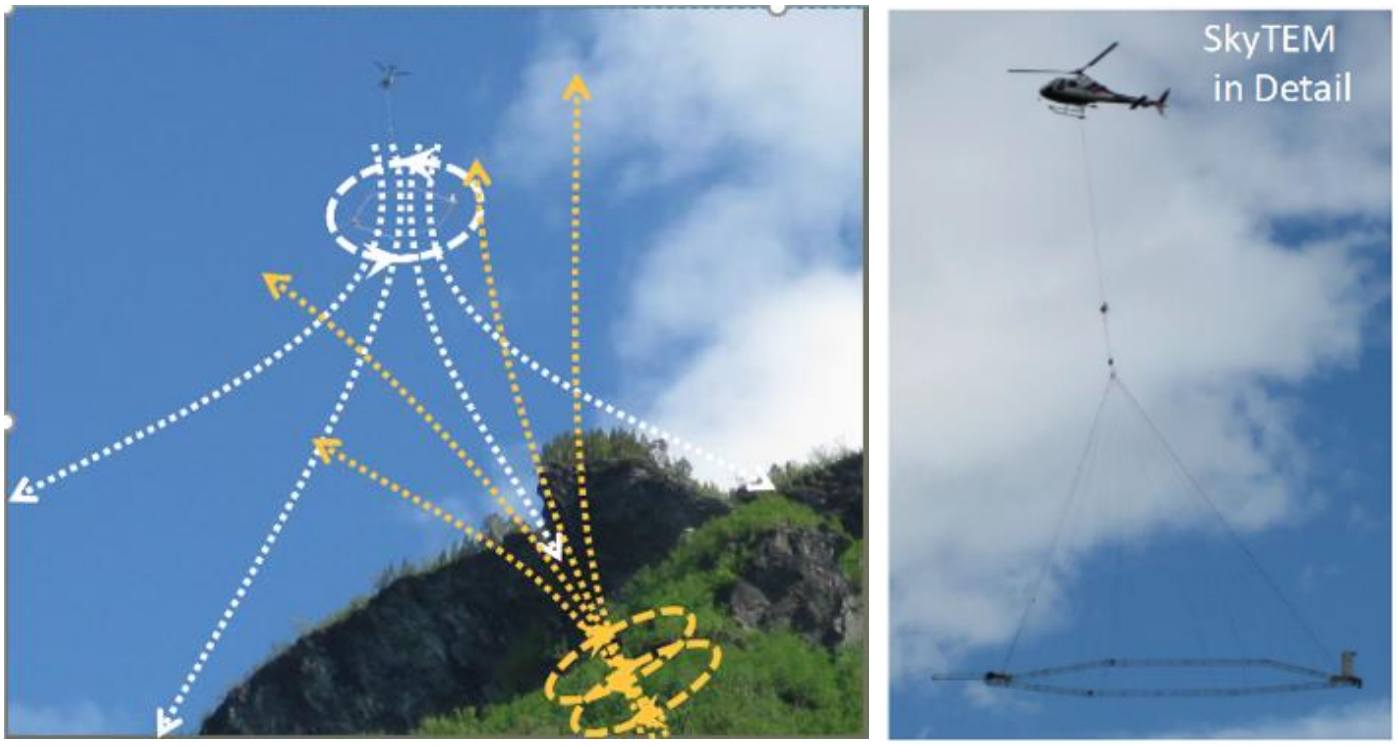

Figure 38. Principle and operation of AEM in the field (left) Eddy currents induced in conductive ground (rights) scanning with helicopter (adapted from Pfaffhuber (2014))

[3] www.emerald-geomodelling.com

Figure 39 shows an example of 3D model generated from AEM scanning from spring 2021 by Emerald Geomodelling for a road-railway project (FRE16 – Ringeriksbane railway and E16 road project). The data was processed with machine learning to detect quick clay near Storelva and Sogna rivers in Norway.

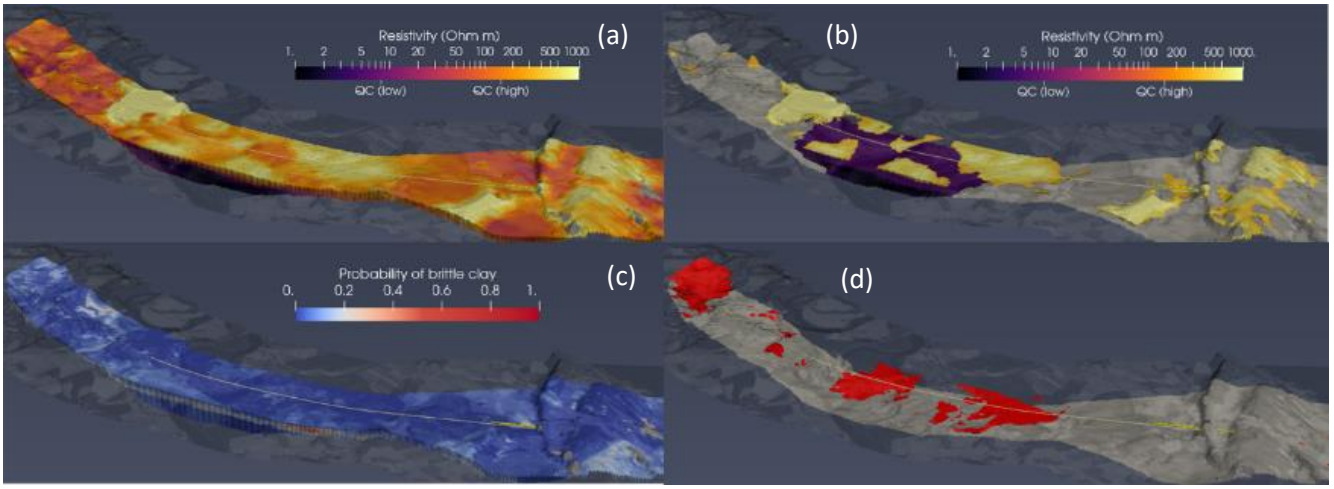

Figure 39. Mapping quick clay with AEM (a)3D volumetric grid of electrical resistivity. (Sediments only; material below bedrock clipped). (b) quick clay (QC) can be ruled out based on resistivity alone where it is very high or very low. (c): Computed probability of weak, sensitive clays are expected based on geophysical and geotechnical data. (d) Extracted volumes where weak, sensitive clays are expected (Source: EMerald Geomodelling)

AEM produces large amounts of data that must be interpreted by specialists. Previously the interpretation was done manually, which was time consuming. In 2015, NGI established an internal expert group for research on artificial intelligence for geotechnical applications. The research has resulted in the development of software which uses machine learning to interpret data generated from the AEM measurements. The software uses so-called Artificial Neural Networks (ANN) to "learn" how the geotechnical engineer performs the interpretation. Based on this, the computer completes the interpretations in the remaining areas with AEM-measurements.

Much research is still needed to optimise the utilisation of AEM for geotechnical work. AEM has potential to reduce costs and offer extensive information but is often limited to "large" infrastructure projects. Though the helicopter or airplane can give access to almost any terrain and location, the accuracy of AEM data in urban areas or near infrastructure need to be investigated further. AEM can produce data with penetration depth up to 300-700 m, though lateral resolution can in many cases be improved with ERT (Pfaffhuber, 2014).

Application of a drone-borne electromagnetic system

Partner: Deltares

Geophysical utilization of drones is a recent and active research topic mainly deploying visible and infrared and radar electromagnetic spectrum. Especially with respect to the magnetic and electromagnetic measurements, no detailed study or data have been presented or published in any academic journals to date. Frequency domain electromagnetic (FDEM) methods on land for local and regional geological, groundwater and geotechnical applications are operational internationally and in The Netherlands since the early eighties (Karaoulis et al., 2020, Ritsema, 1983).

Deltares has investigated the feasibility of executing frequency domain electromagnetic (FDEM) surveys using a commercially available drone. The research to date has focussed on investigating the optimal configuration of drone and electromagnetic instrument, such as the mounting device and distance of the electromagnetic (EM) sensor with respect the drone, the flight altitude, the coil separation and frequency of the EM source, efficiency and safety, the assemblage of instrument and drone data.

The most profound issue that appeared in this research is the importance of altitude control and the distance of the drone from the EM system. It became clear that the drone needed to be separated from the EM systems by a sufficient distance in order to minimize any interference. To avoid drone-instrument interference, it is imperative to design a suitable means of mounting the device, to optimally calibrate the device, to correct for flight elevation variations and to segment and use sounding and horizontal data.

Combining EM sensors and drones fills the gap between ground-based surveys and airborne surveys. While the goal is to avoid the complexity of an airborne survey, some issues directly related to drone-based EM need to be resolved, since there is no “off-the-shelf" system available for this purpose. These issues can be categorized as follows:

1. Noise generated from the drone: in a drone survey the limited payload capacities and engines of a drone forbids too large separation of drone and sensors, but larger separations reduce noise;
2. The height of the sensor above the ground: while it is desirable to have the sensors as close as possible to the ground (typically within 10-20 cm), this is considered unsafe for flying;
3. Elevation: small variations in altitude (e.g. distance to the ground during the flight), generate significant artifacts in the acquired data. To correct and process the data accurately, the height of the drone above the ground always needs to be known accurately; and
4. Data: in a field survey, a very large quantity of data is recorded. Before any interpretation or inversion can be executed all measured data has to be organized. This includes integration of drone, lidar and electromagnetic data sources before data can be enhanced by filtering and recalibration and optionally an altitude correction to the electromagnetic profiling data. Some of the newer EM instruments, record tilt and roll, auxiliary data that can be used to correlate noise originate from instabilities during the flight. It is best to remove these unnecessary, often noisy data.

The results from the field tests of DR-EM at Deltares show that drone-borne electromagnetic (DR-EM) surveying is feasible and high resolution data, comparable to ground surveys and much more detailed than that can be obtained by airborne surveys, can be generated. Above all, an appropriate selection of instrument should match the target depth and a flying strategy should be developed that includes enough sounding recordings to be able to follow instrumental drift and average soil condition for correctional procedures. The survey speed is estimated to be faster that of an FDEM ground survey andit is especially advantageous in poorly accessible terrains.

Applications envisaged, amongst others are: mapping saline water seepage in coastal areas, shallow geological mapping of sand, clay and peat and man-made conductive pipelines water depth, water pollution, subsurface heterogeneities, faults or cavities and man-made underground infrastructures and buried objects, such as UXO’s. Repeated DR-EM surveying will allow for cost-effective monitoring.

4 Imaging technology and image analysis

Evangelia Korre, Ioannis Anastasopoulos

Geotechnical Centrifuge Center, ETH Zurich (Swiss Federal Institute of Technology in Zurich)

Zheng Li, Luc Thorel, Alain Neel, Matthieu Blanc, Thierry Dubreucq

Laboratoire Centrifugeuses Géotechniques GERS-CG, Département Géotechnique, Environnement, Risques Naturels et Science de la Terre (GERS), Université Gustave Eiffel

Sam Stanier, Haitao Lan

Cambridge University Engineering Department, University of Cambridge

4.1 Background

Due to the limitations of the conventional contact measurement methods, i.e. to fix or to attach some sensors to the objects to be observed (either in laboratory or in-situ) (Ko et al. 2021), there is a rising demand of non-contacting/nonintrusive measurement methods, for example, laser, radar, acoustic methods *etc*. In recent years, advanced digital image/vision-based measurement or monitoring using cameras has become increasingly popular. The most popular method for the image-based analysis is Particle Image Velocimetry (PIV), which is often referred to as Digital Image Correlation (DIC) in the field of experimental mechanics.

Particle Image Velocimetry (PIV) is a velocity-measuring technique that was originally developed in the field of experimental fluid mechanics (Adrian 1991). The technique was first implemented using double-flash photography of a seeded flow. The resulting photographs contain image pairs of “reference” and “target” of the distributed seed particles, which are then discretized into sets of test “subsets” or “patches” (the terms are interchangeable and refer to a contiguous group of pixels within the digital image). The displacement vector of each subset during the interval between the flashes is found by locating the peak of the cross-correlation function between the reference and target images. The peak in the cross-correlation function indicates that the reference and target images of each seeding particle captured during the flashes are overlying each other, and the correlation offset is then equal to the displacement vector. The time elapsed between the reference and target images allows the velocity of the subsets to be determined from the inferred displacements.

As described in detail in White et al. (2003), for the case of geotechnical model testing, the fundamental principles of PIV are slightly modified, due to the natural texture of soil and the addition of distinguishable “texture” or “contrast” on the soil surface (e.g. colored sand, targets embedded in the soil surface, etc.) and the fact that instantaneous deformations are generally of more interest than velocities. Digital images are captured either directly with a digital camera or by extracting frames from an analogue video signal (White et al. 2003), where the frame capture rate is dependent upon the type of behavior being observed; quasi-static experiments typically use low frame rates of the order of 0.1 Hz, whereas in dynamic tests the frame rate required is usually significantly higher (at least 1000 Hz) to prevent aliasing of the measurements. The images acquired typically capture a two-dimensional plane of the soil within the geotechnical model by viewing a cross-section of the model via a glass or acrylic window. Once a

series of images have been captured, they are analyzed using one of two main genera of PIV/DIC algorithms:

- Cross-correlation peak fitting algorithms; and
- Iterative algorithms.

The cross-correlation peak fitting algorithms operate by first obtaining the integer pixel offset of the peak of the cross-correlation function. This gives the displacement components of the subset to the nearest integer pixel, which is then refined to sub-pixel precision, typically, by fitting a bi-cubic surface to the peak of the cross-correlation function and its eight nearest neighbours. Such an approach is referred to as a "zeroth-order" method since the subset translates only vertically and horizontally and any deformation (including rotation) is ignored. In the geotechnical field a classical example of a "zeroth-order" approach – the MATLAB package GeoPIV – is described byWhite et al. (2003).

The iterative algorithms use the same integer pixel estimate of the displacements to pre-condition a Newton-Raphson or Gauss-Newton algorithm, which attempts to solve the unknowns in a "shape" or "warp" function that describes the displacement and potentially also the deformation of the subset (Pan et al. 2008). Iterative methods involving shape functions that include the first and second derivative of the displacements of the subset are sometimes referred to as "first-order" and "second-order" methods (Lu and Cary, 2000). The addition of the derivatives of the displacements facilitates rotation of the subsets and significant deformation with minimal loss of correlation. The order of solution of the subsets within the image series typically begins with a "seed" subset in a region of the reference image known to experience minimal deformations. The solution of the remaining subsets can then proceed using a so-called "reliability-guided" approach where the current subset deformation is pre-conditioned using the nearest neighbour with highest correlation (Pan, 2009). In the geotechnical field a recent example of a first-order reliability-guided approach – the MATLAB package GeoPIV-RG – is described by (Stanier et al., 2016b).

Cross-correlation peak fitting methods are prone to so-called "peak-locking" errors when the subset texture is not optimal, resulting in displacements biasing towards integer pixel values due to a breakdown in the sub-pixel refinement process. This breakdown can result in erroneous apparent "localization" of deformation when strains are computed from the derivatives of the displacement field determined via PIV/DIC. Iterative algorithms appear to be significantly more robust and less impact by this problem (Stanier et al., 2016a).

The PIV/DIC approach has been proven to be a more accurate and cost-efficient method of image analysis compared to previous image-based techniques such as x-ray tomography (Butterfield et al. 1970; Paikowsky and Xi 2000), especially given that digital camera technology is now extremely cheap. Measurements are derived in pixel units, initially, and are typically converted to real world units via photogrammetric correction techniques that can account for camera lens and pose induced distortion(White et al., 2003). Optimal precision measurements can only be derived via PIV/DIC methods using images with:

- Sharply focused images;
- Even and temporally consistent illumination;
- Optimised image texture.

A general guide to model setup in order to achieve the above three requirements is given by Stanier et al. (2016a).

The techniques described thus far can also be applied to three-dimensional surfaces, such as the free-surface of geotechnical centrifuge sample. Sinha et al. (2021) describes an interesting application of a three-dimensional image-based approach in centrifuge tests through using high-speed Photron cameras

and the TEMA Classic 3D software at the Center for Geotechnical Modeling (CGM) at University of California, Davis (UCD). The cameras and their mounting, as well as the target markers, lighting, camera calibration, and camera triggering are described, followed by a discussion on the software options selected for the analysis of videos recorded for a centrifuge model test conducted on the 9 m-radius centrifuge. The approach operates by finding the locations of discrete targets in each of an array of cameras positioned in slightly different positions. Then, using stereo-photogrammetric techniques the position of each marker can be determined in three dimensions. The results presented show that the PIV/DIC method is effective and reliable in obtaining the positions, displacements, velocities, and accelerations of the targets. In addition to using discrete targets on the soil surface, "structure-from-motion" or "SfM" techniques can also be used to monitor full-field settlements by utilizing natural image texture and feature detection algorithms (Eichorn & Haigh, 2019).

4.2 Particle Image Velocimetry

Utilizing image analyses in tsunami study

Partner: ETH-Zurich

Several experimental campaigns at ETH-Zurich have utilized the PIV methodology as an image analysis technique in order to measure deformations during testing a geotechnical model. For example, Jones and Anastasopoulos (2021) utilized PIV to determine the deformations inside a soil model, subjected to tsunami loading (Figure 40).

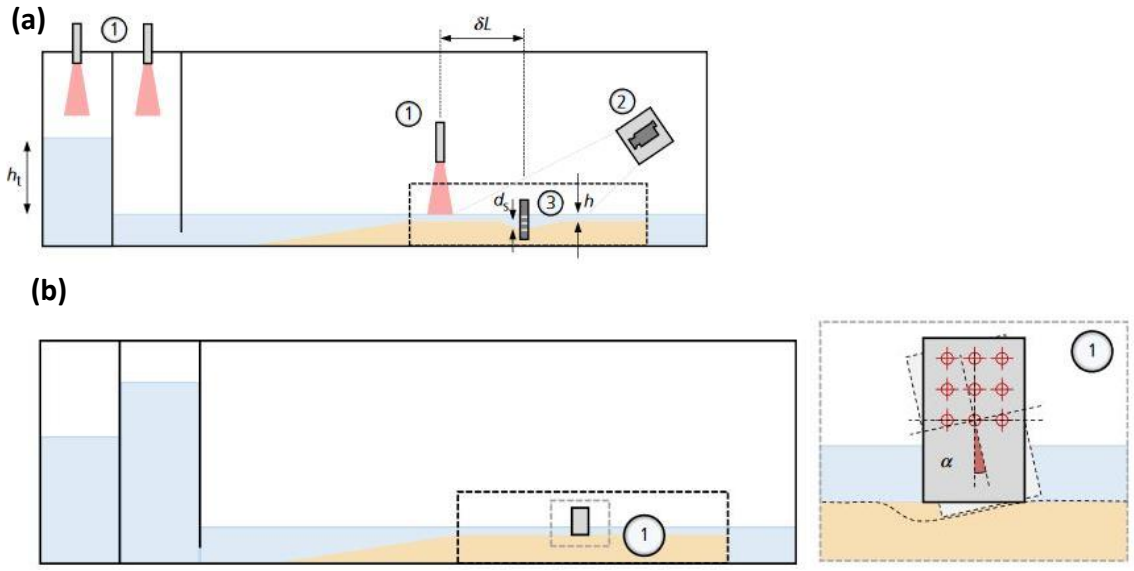

Figure 40. Experimental set-up used for scour experiments, (b) Illustration of the employed scheme for image analysis (adapted from Jones and Anastasopoulos (2021)).

An alternative methodology of image analysis is to use an appropriate software, such as the motion tracking software TEMA Automotive Lite3.5–016 by Image Systems. Image analysis was employed by tracking with a high-speed camera at a rate of 1000 Hz the area of interest on the soil surface, where cut cable-tie heads were embedded and served as targets (Kokkali et al., 2018, Korre et al., 2020) (Figure 41). The camera was setup to capture pre-triggering information while the centrifuge was in flight, such that as soon as the data acquisition system was triggered, the high-speed camera was automatically triggered, thus synchronizing the captured video with the data from other sensors. The recorded slow-motion video was then imported into the TEMA software and processed. This particular software operates by comparing the boundaries of objects between multiple frames and directly providing absolute

displacement, velocity, and acceleration time histories (Kokkali et al. 2018). The geometrical correlation between the dimensions in the model and in the video was facilitated by providing in the software the distance between two stationary points in the model. In this way, the scaling factor to correlate model distance to pixels was determined – so-called "linear scaling".

The comparative advantage of this "more automated" method of image analysis is that the user maintains a view of the tracked video while the analysis is progressing. In this way, the user can immediately intervene and adjust the settings accordingly in case light reflections or other distortions affect the quality of tracking.

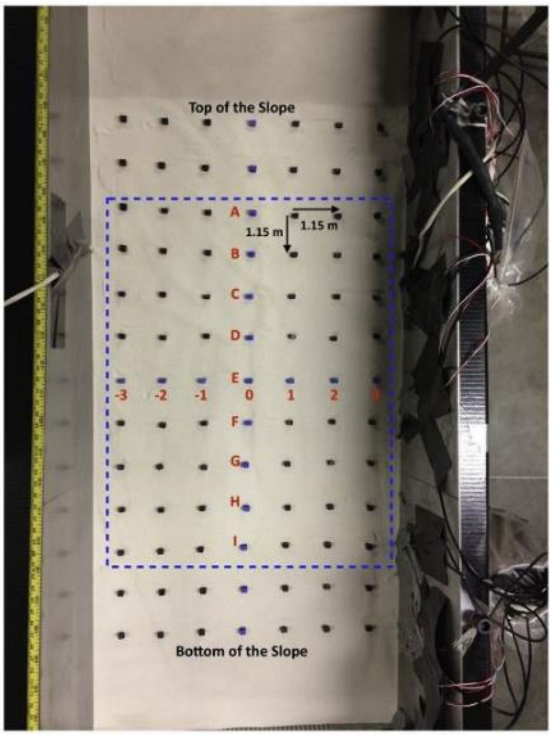

Figure 41. Grid of targets used for tracking with the high-speed camera. The blue dashed frame indicates the area tracked by the high-speed camera. Adapted from Korre et al. (2020).

Application of PIV/DIC in pile and embankment study

Partner: Université Gustave Eiffel

Image/vision-based correlation analyses have been carried out and applied to several recent centrifuge tests at the Université Gustave Eiffel – Campus de Nantes (formerly IFSTTAR). This section briefly presents two examples to demonstrate the potential application of DIC in centrifuge model tests.

2D DIC analysis for centrifuge model of pile installation

The first DIC analysis was carried out for analyzing the strain field of the penetration of a pile into sand. The centrifuge test was performed in a 2D soil container consisting of a transparent window which enables observation of the penetration process by a digital camera. The DIC analysis was carried out using TEMA software. As shown in Figure 42 (left), a DIC zone was assigned at the vicinity of the penetration location. The DIC analysis zone is limited near the penetration point in order to save the computational efficiency. The strain field ε_1 is shown in Figure 42 (right). It is clear that the strain localization is observed at the penetration point.

3D image-based motion analysis

Besides the above presented 2D DIC analysis, as previously noted, the method is also applicable to capture 3D motions. A test of the 3D motion analysis was carried out on a centrifuge test of embankment subjected to base shaking. As shown in Figure 43, two cameras were installed with a certain angle of separation above the embankment. In order to capture the feature points and to facilitate the 3D motion tracking, markers were added on the surface of the embankment (on the top and the slope), as shown in Figure 43. After the test, the recorded video was analyzed using TEMA software, as shown in Figure 44.

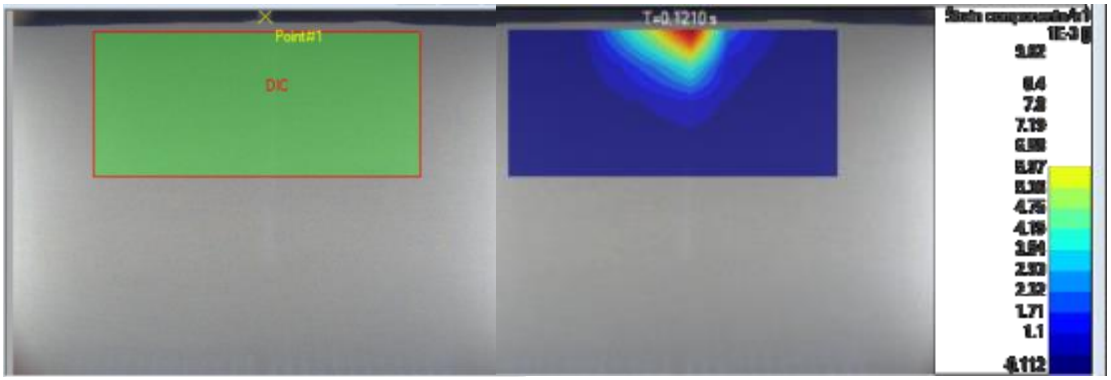

Figure 42 Digital image correlation analysis of the strain field of a centrifuge test on pile penetration

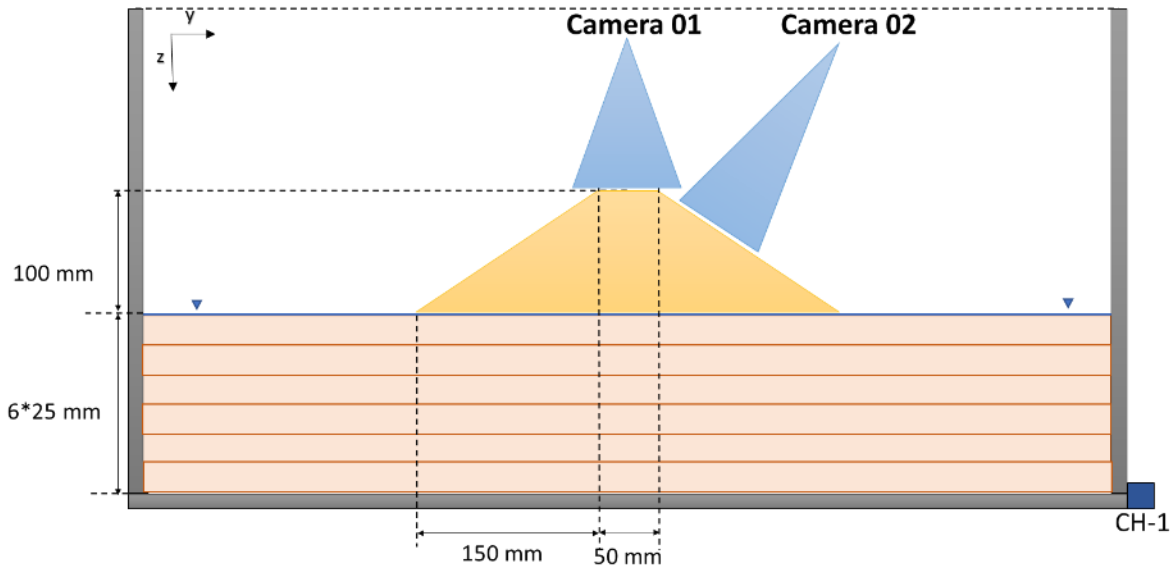

Figure 43. Cameras for monitoring the settlement of a centrifuge model of an embankment (unit in model scale)

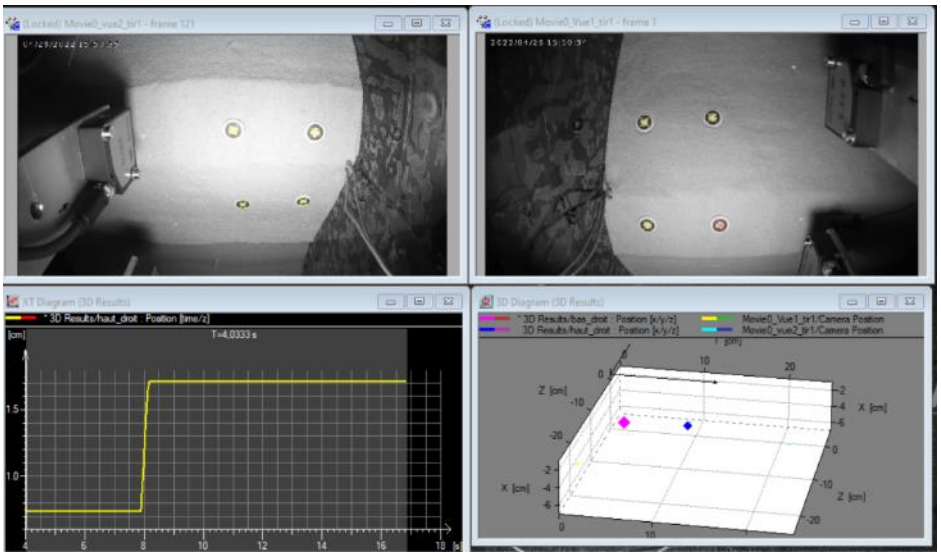

Figure 44. Image-based motion analysis by TEMA image system

The result obtained by image-based motion tracking was compared with the data measured by the conventional laser capture. Figure 45 shows that a reasonable agreement was obtained between the two methods.

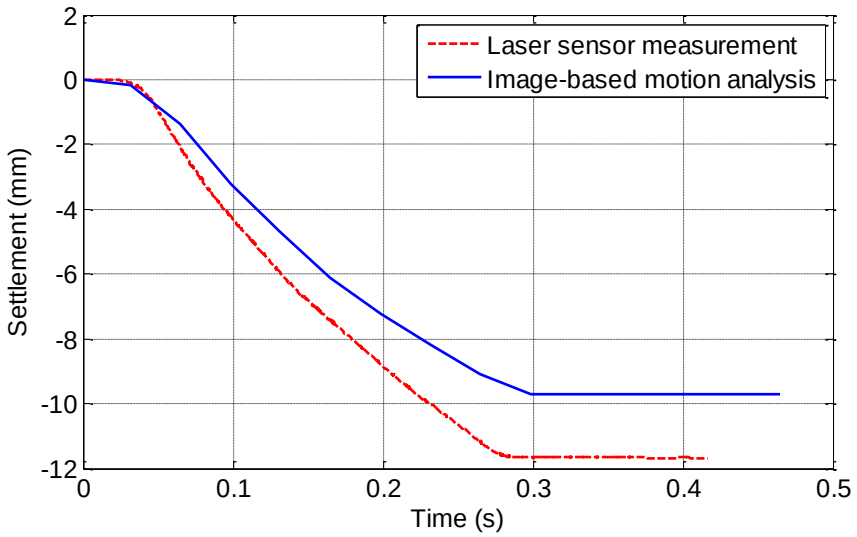

Figure 45. Comparison of the results between the image analysis and the conventional measurement

However, there are also some problems in applying the image-based analysis to the centrifuge test. For example, the calibration of the camera lens taking into the deformation of the supporting system under macro-gravity is a challenge, especially for the calibration for 3D cases. For the dynamic centrifuge test, the vibration caused by the shaking table can also influence the precision of the image analysis. It is also found that the uneven lighting may also influence the reliability of measurements that can be derived using PIV/DIC approaches.

Application of PIV/DIC and SfM in offshore geotechnics

Partner: University of Cambridge

Subsea cable breakout using adaptively refined PIV/DIC

A recent project using PIV/DIC at the University of Cambridge has involved observing the breakout of buried cables at 1g in Hostun sand. A new Python PIV/DIC code – called geopyv and soon to be released on PyPI– has been developed, which can automatically refine the topology of the mesh such that small subset spacing is utilised in regions experiencing large deformations and large spacing is utilised in regions experiencing minimal deformations. An example of the output is shown in Figure 46 in the form of a shear strain field.

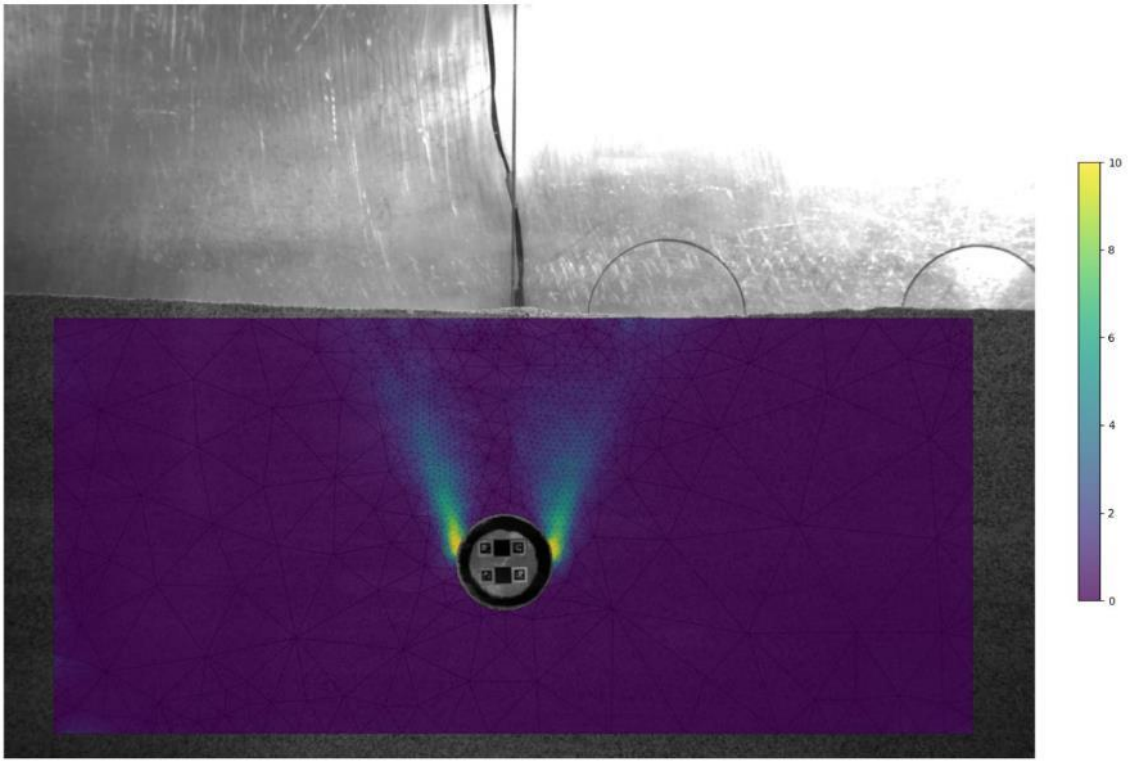

Figure 46. Adaptively refined mesh topology for subsea cable breakout experiments

The development of such adaptive PIV/DIC algorithms allows the influence of measurement noise to be minimised, potentially opening up the possibility of full-field image-based constitutive model calibration (e.g. Charles et al. (2018)), where parasitical work caused by measurement noise imposes a serious limitation on the scope of usage of PIV/DIC derived measurements.

Slope failure around a buried pipeline using SfM

Eichhorn and Haigh (2019) used SfM to monitor the deformation of a slope with a buried pipeline at 400g in the drum centrifuge at the University of Cambridge. The system they developed used an array of Raspberry Pi Zero W computers and cameras to capture images of the slope from various vantage points

(see Figure 47). SfM algorithms in the Agisoft Metashape package were used to extract the three-dimensional shape of the slope before and after failure, as shown in Figure 48, which shows the influence of the pipeline on restraining the slope failure.

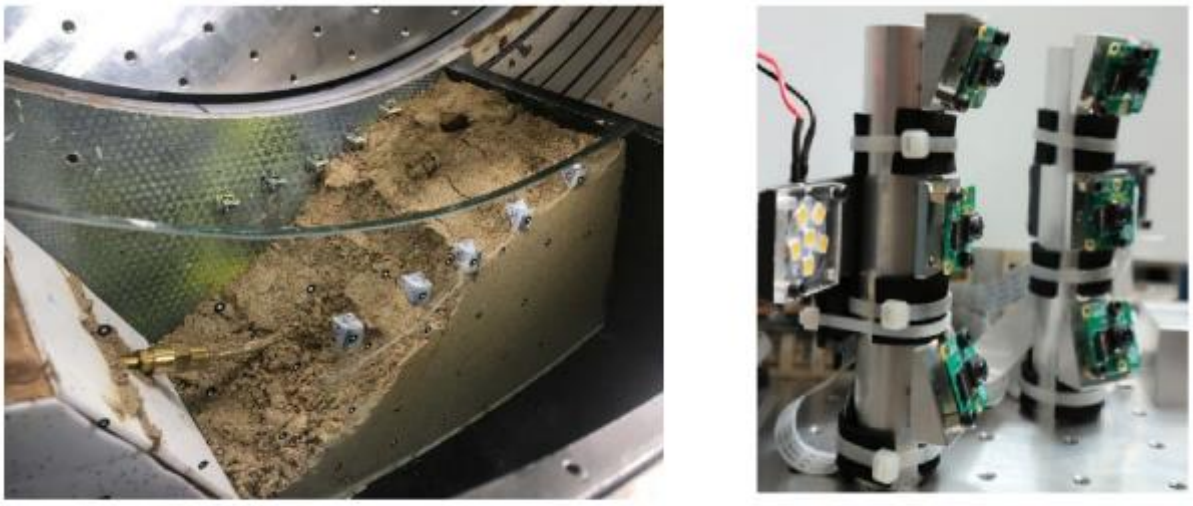

Figure 47. Photographs of (a) the centrifuge model slope post-landslide and (b) the Raspberry Pi multi-camera photogrammetry system, after Eichorn and Haigh (2019)

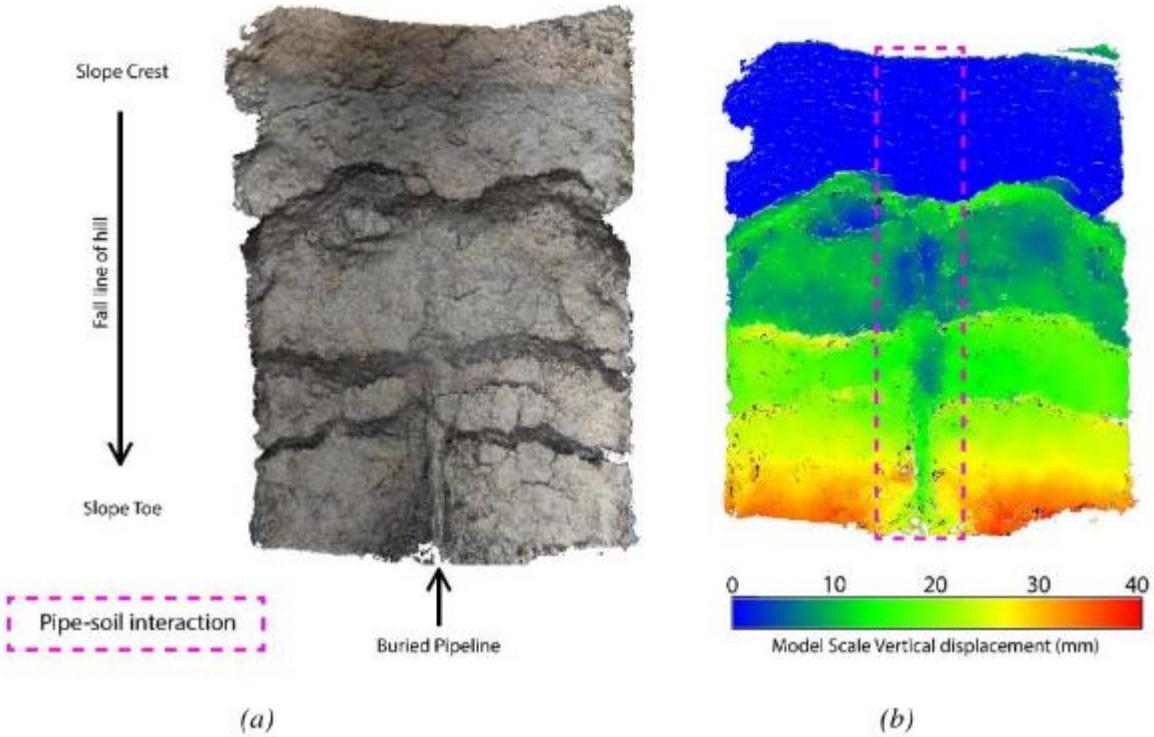

Figure 48. (a) 3D point cloud of landslide surface, and (b) vertical displacement raster map showing model scale movements from un-deformed slope to post-failure surface, after Eichorn and Haigh (2019)

5 Summary, recommendations and conclusions

Climate change, extreme events and aging are causing and/or accelerating numerous geotechnical challenges such as geohazards and deformation/settlement of buildings and infrastructure. In addition, increasing demand and pressure on the built environment stimulate the need for innovative methods/equipment for characterization of ground condition and detection of objects, utilities, defects which can interfere with construction/maintenance of infrastructure. Remote sensing, geophysical methods and imaging technology offer great potential for effective and cost-efficient approaches for monitoring critical infrastructure, characterization of sub-surfaces and detection of objects, defects and utilities. Their main advantages are non-intrusive/non-destructive, fast and the possibility to cover large areas and challenging terrain which are costly or impossible to measure if using traditional methods.

Many GEOLAB partners had or have ongoing research and development activities which utilize one or more remote sensing, geophysical methods or imaging technology in innovative physical modelling, small laboratory experiment, medium lab-field test or large/full-scale field testing. Table 3 shows a summary of research activities in remote sensing, geophysical method and imaging technology performed in the past or at the present by GEOLAB partners to study various geotechnical challenges. Except to Particle Image Velocimetry - PIV, these technologies have reached TRL 6-7, thus they have been or are applicable in real operational environment. Some of the example applications presented in this report are performed in practical industry projects (e.g. road construction, dam monitoring).

Table 3. Summary of typical research activities in remote sensing, geophysics and imaging technology conducted by GEOLAB partners to address various geotechnical challenges.

Geotechnical challenges	Applicable technology	TRL
Monitoring of deformation and settlement of buildings and infrastructures	Remote sensing (e.g. InSAR, LiDAR)	6-7
Physical modelling of deformation and settlement in centrifuges	Image analysis (e.g. Particle Image Velocimetry)	4-5
Monitoring of landslide and other geohazards	Remote sensing (e.g. InSAR, LiDAR)	6-7
Detecting of objects, utilities, defects…etc	Geophysical methods (e.g. Electrical Resistivity Tomography - ERT, Ground Penetrating Radar – GPR)	6-7
Soil characterisation	Geophysical methods (e.g. Electrical Resistivity Tomography - ERT, seismic survey, Electromagnetic survey- EM)	6-7

There is however much need for more modelling in the laboratory and testing in the field as well as research in data processing to optimize their applicability in geo-engineering challenges. There is in addition a need for more real cases to demonstrate the advantages and cost-effectiveness of these methods to encourage their uses in practice.

Table 4 presents some recommendation for future research activities in remote sensing, geophysics and imaging technology based on current state-of-art of GEOLAB consortium to push for technological advances, innovation and collaboration within GEOLAB community. There is great potential for innovation through collaborative research among GEOLAB partners as well as with external users through activities such as Transnational Access. More cross-disciplinary collaboration between geotechnicians and geophysicists are in addition essential to ensure technological advances adapted in practice. Activities in GEOLAB and related research activities by GEOLAB partners will nurture such collaboration.

Table 4. Recommendations on future research activities to promote technological advances, innovations and collaborations within GEOLAB consortium and community beyond the state-of-art.

Geotechnical challenges	Possible future research activities	TRL
Monitoring of deformation and settlement of buildings and infrastructures	• Improvement in filtering out noises from remote sensing measurements (e.g. from water, vegetation) • Advancement in accuracy and robustness of low-cost ground-based LiDAR and/or radar for monitoring applications	6-7
Physical modelling of deformation and settlement in centrifuges	• Full-field image-based model constitutive model calibration by adaptive Particle Image Velocimetry (PIV)	4-5
Monitoring of landslide and other geohazards	• Advancements in detecting capability of remote sensing technologies (e.g. InSAR, LiDAR) with future satellites (e.g. ESA satellite Rose-L (Sentinel-12)) with more frequent coverage. • Application of remote sensing to new types of landslides (e.g. quick clay landslide)	6-7
Detecting of objects, utilities, defects…etc	• Extending applications of geophysical methods (e.g. GPR, ERT) to new applications (e.g. utilities with different material properties) • Reduction of noises and disturbances in GPR, ERT measurements	6-7
Soil characterisation	• Improved characterisation of challenging soils (e.g. soft clay, quick clay) with geophysical methods (e.g. Electrical resistivity tomography - ERT, seismic survey, electromagnetic survey- EM) • Probabilistic methods and use of machine learning for analysing data for geophysical survey for characterisation problem.	6-7

6 References

BERARDINO, P., FORNARO, G., LANARI, R. & SANSOSTI, E. 2002. A new algorithm for surface deformation monitoring based on small baseline differential SAR interferograms. *IEEE Transactions on Geoscience and Remote Sensing,* 40**,** 2375-2383.

CHARLES, J., SMITH, C. & BLACK, J. Identification of soil stress-strain response from full field displacement measurements in plane strain model tests. 9th International Conference on Physical Modelling in Geotechnics, 2018 17-20 Jul 2018, London, UK.

COULIER, P., CUÉLLAR, V., DEGRANDE, G. & LOMBAERT, G. 2015. Experimental and numerical evaluation of the effectiveness of a stiff wave barrier in the soil. *Soil Dynamics and Earthquake Engineering,* 77**,** 238-253.

EICHHORN, G. & HAIGH, S. Imaging of landslide-pipeline interaction in a geotechnical drum centrifuge. 2nd International Conference on Natural Hazards & Infrastructure, ICONHIC2019, 2019 23-26 June, 2019, Chania, Greece.

EMERALD GEOMODELLING. 2022. *Identified Risks: Soil types; Bedrock topography, Hazardous rock type, Major weakness zones* [Online]. EMerald Geomodelling. Available: www.emerald-geomodelling.com [Accessed 17.08.2022].

FERRETTI, A., PRATI, C. & ROCCA, F. 2000. Nonlinear subsidence rate estimation using permanent scatterers in differential SAR interferometry. *IEEE Transactions on Geoscience and Remote Sensing,* 38**,** 2202-2212.

GEOSCIENCE AUSTRALIA. 2022. *Airborne Electromagnetics* [Online]. Available: https://www.ga.gov.au/scientific-topics/disciplines/geophysics/airborne-electromagnetics [Accessed 16.08.2022 2022].

GIARDINA, G., MILILLO, P., DEJONG, M. J., PERISSIN, D. & MILILLO, G. 2019. Evaluation of InSAR monitoring data for post-tunnelling settlement damage assessment. *Structural Control and Health Monitoring,* 26**,** e2285.

HALDAR, S. K. 2018. Chapter 6 - Exploration Geophysics. *In:* HALDAR, S. K. (ed.) *Mineral Exploration (Second Edition).* Elsevier.

HANSSEN, R. F. 2001. *Radar Interferometry: Data Interpretation and Error Analysis.,* Dordrecht, the Netherlands, Springer Science + Business Media.

HEIKKINEN, E. & KANTIA, P. 2011. Suitability of Ground Penetrating Radar for Locating Large Fractures. Eurajoki, Finland: Posiva OY.

JEBUR, M. N., PRADHAN, B. & TEHRANY, M. S. 2014. Detection of vertical slope movement in highly vegetated tropical area of Gunung pass landslide, Malaysia, using L-band InSAR technique. *Geosciences Journal,* 18**,** 61-68.

JONES, L. & ANASTASOPOULOS, I. 2021. Miniaturised tsunami generator to model interaction of tsunami with coastal infrastructure. *International Journal of Physical Modelling in Geotechnics,* 21**,** 135-149.

KARAOULIS, M., RITSEMA, I., BREMMER, C. & KLEINE, M. 2020. *Drone-Borne Electromagnetic (DREM) Surveying in The Netherlands*.

KOKKALI, P., ABDOUN, T. & ZEGHAL, M. 2018. Physical modeling of soil liquefaction: Overview of LEAP production test 1 at Rensselaer Polytechnic Institute. *Soil Dynamics and Earthquake Engineering,* 113**,** 629-649.

KORRE, E., ABDOUN, T. & ZEGHAL, M. 2020. Liquefaction of a sloping deposit: LEAP-2017 centrifuge tests at Rensselaer Polytechnic Institute. *Soil Dynamics and Earthquake Engineering,* 134**,** 106152.

L'HEUREUX, J.-S., LINDGÅRD, A. & EMDAL, A. 2019. The Tiller-Flotten research site: Geotechnical characterization of a very sensitive clay deposit. *AIMS Geosciences,* 5**,** 831-867.

LACASSE, S., L'HEUREUX, J.-S. & LIU, Z. 2022. Keynotes: Reducing landslide risk - Emerging challenges and novel technologies. *Georisque VIII - Geohazards 8.* Quebec, Canada: The Canadian Geotechnical Society.

LEIJEN, F. V. 2014. *Persistent Scatterer Interferometry based on geodetic estimation theory.* PhD Thesis, Technical University Delft.

LU, H. & CARY, P. D. 2000. Deformation measurements by digital image correlation: Implementation of a second-order displacement gradient. *Experimental Mechanics,* 40**,** 393-400.

MACCHIARULO, V., MILILLO, P., BLENKINSOPP, C. & GIARDINA, G. 2022. Monitoring deformations of infrastructure networks: A fully automated GIS integration and analysis of InSAR time-series. *Structural Health Monitoring,* 21**,** 1849-1878.

MEADE, S. 2021. *Stream Bank Erosion: Applications of Remote Sensing* [Online]. Available: https://storymaps.arcgis.com/stories/c8d3b89a56fa4c56bc3cee16c586680b/print [Accessed 31.10.2021].

MILILLO, P., GIARDINA, G., PERISSIN, D., MILILLO, G., COLETTA, A. & TERRANOVA, C. 2019. Pre-Collapse Space Geodetic Observations of Critical Infrastructure: The Morandi Bridge, Genoa, Italy. *Remote Sensing,* 11**,** 1403.

MILILLO, P., RIEL, B., MINCHEW, B., YUN, S. H., SIMONS, M. & LUNDGREN, P. 2016. On the Synergistic Use of SAR Constellations' Data Exploitation for Earth Science and Natural Hazard Response. *IEEE Journal of Selected Topics in Applied Earth Observations and Remote Sensing,* 9**,** 1095-1100.

NGU. 2022. *Terrestrial Laser Scanning* [Online]. Geological Survey of Norway. Available: https://www.ngu.no/en/topic/terrestrial-laser-scanning [Accessed 14.08.2022].

NISHIGUCHI, T., TSUCHIYA, S. & IMAIZUMI, F. 2017. Detection and accuracy of landslide movement by InSAR analysis using PALSAR-2 data. *Landslides,* 14**,** 1483-1490.

PAN, B. 2009. Reliability-guided digital image correlation for image deformation measurement. *Applied Optics,* 48**,** 1535-1542.

PFAFFHUBER, A. A. 2014. Final Seminar: Remote Mapping and Warning. Norwegian Geotechnical Institute.

REVIL, A. & JARDANI, A. 2010. Stochastic inversion of permeability and dispersivities from time lapse self-potential measurements: A controlled sandbox study. *Geophysical Research Letters,* 37.

RITSEMA, I. L. 1983. Electromagnetic resistivity profiling for the determination of lateral variation in lithology or ground water quality. *MIIGS* Noordwijker Hout, NL: Unesco Proceedings.

SCHLÖGL, M., GUTJAHR, K. & FUCHS, S. 2022. The challenge to use multi-temporal InSAR for landslide early warning. *Natural Hazards,* 112**,** 2913-2919.

SETCHELL, S., AZAHAR, M., RUSLI, Q. N. & LOWE, N. 2016. *The use of Non-Invasive Geophysical Techniques to build 3-Dimensional ground models and reduce the cost and risk of site investigation*.

SHIN, Y., CHOI, J. C., QUINTEROS, S., SVENDSEN, I., #039, HEUREUX, J.-S. & SEONG, J. 2020. Evaluation and Monitoring of Slope Stability in Cold Region: Case Study of Man-Made Slope at Øysand, Norway. *Applied Sciences,* 10**,** 4136.

SILVAST, M., ERVELÄ, O. & LEPPÄLÄ, A. 2019. Preliminary Report on Subsurface Defects Detection Solution for Railway Tunnels.

SILVAST, M., ERVELÄ, O. & LEPPÄLÄ, A. 2021. Tunnel validation Report.

SILVAST, M., NURMIKOLU, A., WILJANEN, B. & LEVOMÄKI, M. 2013a. Identifying frost-susceptible areas on Finnish railways using the ground penetrating radar technique. *Proceedings of the Institution of Mechanical Engineers, Part F: Journal of Rail and Rapid Transit,* 227**,** 3-9.

SILVAST, M., NURMIKOLU, A., WILJANEN, B. & MÄKELÄ, E., . IN PROCEEDINGS, , , . INTERNATIONAL HEAVY HAUL ASSOCIATION CONFERENCE, VOL. 1, , PP. Efficient track rehabilitation planning by integrating track geometry and GPR data. 10th International Heavy Haul Association Conference, February 4-6, 2013, 2013b New Delhi, India. International Heavy Haul Association IHHA, 154-159.

STANIER, S., DIJKSTRA, J., LEŚNIEWSKA, D., HAMBLETON, J., WHITE, D. & MUIR WOOD, D. 2016a. Vermiculate artefacts in image analysis of granular materials. *Computers and Geotechnics,* 72**,** 100-113.

STANIER, S. A., BLABER, J., TAKE, W. A. & WHITE, D. J. 2016b. Improved image-based deformation measurement for geotechnical applications. *Canadian Geotechnical Journal,* 53**,** 727-739.

SUTARTO, T. 2014. *Airborne Lidar Technique for Topographic Mapping: An Application in Streambank Erosion Measurement*.

TIJERA, A., ASANZA, E., RUIZ, R. & RUIZ, J. M. 2019. Geophysical and geotechnical characterization of soft marine soils in port infrastructures. *XVII European Conference on Soil Mechanics and Geotechnical Engineering, ISSMGE.* Reikiavik, Ireland.

TIJERA, A., ASANZA, E., RUIZ, R. & RUIZ, J. M. 2020. Aplicación de técnicas geofísicas para la caracterización de suelos marinos y rellenos en infraestructuras portuarias. *Boletín de la Sociedad española de mecánica del suelo e ingeniería geotécnica,* 203**,** 2-14.

USGS. 2022. *Mapping, Remote sensing, and Geospatial data* [Online]. U.S. Geological Survey. Available: https://www.usgs.gov/ [Accessed 13.08.2022].

VÖGE, M., FRAUENFELDER, R., SALAZAR, S., TORGERSRUD, Ø. & PICIULLO, L. 2022. INSAR displacement monitoring on tailings storage facilitie. *International Geoscience and Remote Sensing Synposium (IGARSS 2022).* Kuala Lumpur, Malaysia: IEEE - GRSS (Geosicence and remote sensing society).

WHITE, D. J., TAKE, W. A. & BOLTON, M. D. 2003. Soil deformation measurement using particle image velocimetry (PIV) and photogrammetry. *Géotechnique,* 53**,** 619-631.

WHITE, J., HURLEBAUS, S., SHOKOUHI, P., WITTWER, A. & WIMSATT, A. 2014. Noncontact techniques for monitoring of tunnel linings. *Structural Monitoring and Maintenance,* 1**,** 197-211.

WIMSATT, A., J., W., LEUNG, C., SCULLION, T., HURLEBAUS, S., ZOLLINGER, D., GRASLEY, Z., NAZARIAN, S., AZARI, H., YUAN, D., SHOKOUHI, P., SAARENKETO, T. & F., T. 2013. Mapping Voids, Debonding, Delaminations, Moisture, and Other Defects Behind or Within Tunnel Linings. Washington, D.C., USA.

ZAN, Y., LI, Z., SU, G. & ZHANG, X. 2016. An innovative vehicle-mounted GPR technique for fast and efficient monitoring of tunnel lining structural conditions. *Case Studies in Nondestructive Testing and Evaluation,* 6**,** 63-69.